AN ANALYSIS OF AN ELECTROMECHANICAL ANALOGUE COMPUTING SYSTEM

J. L. MILES

THESIS
M585

Library
U. S. Naval Postgraduate School
Monterey, California

AN ANALYSIS OF AN ELECTROMECHANICAL ANALOGUE COMPUTING SYSTEM

By

Jack Leroy Miles
First Lieutenant, U. S. Marine Corps

ESSAY

SUBMITTED TO THE ADVISORY BOARD

OF THE

SCHOOL OF ENGINEERING

THE JOHNS HOPKINS UNIVERSITY

IN CONFORMITY WITH REQUIREMENTS

FOR THE DEGREE OF MASTER OF SCIENCE

IN ENGINEERING

Baltimore

1 9 5 2

Thesis
M545

ACKNOWLEDGEMENT

The author gratefully expresses his indebtedness to Mr. Fletcher C. Paddison for his unfailing cooperation and encouragement throughout the progress of the test; to Dr. Walter A. Good and Dr. John M. Kopper for their guidance and helpful discussions; to Mr. Loran A. Wenrich and Mr. Alan A. Hamilton for their laboratory assistance and cooperation in securing components; and to his wife for the preparation and typing of this paper.

18050

TABLE OF CONTENTS

Acknowledgement ii

Table of Contents iii

1. INTRODUCTION 1

2. THEORY 4

2.1 Basic Configuration 4

2.2 The Differential Equation to be Solved 4

2.3 Determination of the System Transfer Function by Dynamic Analysis 5

2.4 Determination of the Overall System Transfer Function by Servo Analysis.. 8

2.5 Theoretical Development of the Expressions for the Amplitude Ratio and the Phase Shift for a Second Order System 12

2.6 The Interrelationships of the Constant Coefficients and the System Parameters of Damping Ratio and the Undamped Natural Frequency 14

2.7 Calculated Results from the Expressions for the Amplitude Ratio and the Phase Shift Versus the Input Frequency ... 16

2.8 Development of Expressions for the Amplitude Ratio and Phase Shift for a Third Order System 20

3. EXPERIMENTAL PROCEDURE AND RESULTS.....22

3.1 Descriptions of Components 22

3.2 Computer Calibration and Operation 31

3.3 Establishing the Linear Limits 41

3.4 The Closed-Loop System and Measuring Apparatus.....57

3.5 The Experimental Results 65

4. CORRELATION OF THE EXPERIMENTAL AND THEORETICAL RESULTS.....75

4.1 Experimental versus Second-Order Theory.....75

4.2 Experimental versus Third-Order Theory.....76

5. ISOLATION OF THE ADDITIONAL DELAY.....81

5.1 Discussion of Delay.....81

5.2 Experimental Procedure.....83

5.3 Correlation of Results.....91

6. CONCLUSIONS AND RECOMMENDATIONS.....92

APPENDIX A: Symbols.....94

APPENDIX B: Solution of the Equation of Motion.....96

BIBLIOGRAPHY.....99

VITA.....100

AN ANALYSIS OF AN ELECTROMECHANICAL ANALOGUE COMPUTING SYSTEM

1. INTRODUCTION

The object of this investigation was to conduct an experimental analysis and prepare a documented study of the functioning of an electromechanical analogue computing system. It was the purpose thereby to establish the frequency range over which the system operates effectively, to discover and evaluate any additional time delays heretofore unknown, and to reveal any discrepancies in the present method of utilizing the system.

The computing system described and analyzed herein was developed because of the need of an instrument or device to solve a particular differential equation. It was necessary to construct an electromechanical computer of the analogue type to simulate the rolling motion of a body in space rotating about its longitudinal axis. The equation of motion can then be represented by a linear second order differential equation with constant coefficients, where the coefficients are functions of the dynamic characteristics of the particular test vehicle.

The experimental results were obtained by varying the frequency of the sinusoidal input signal and studying the phase lag of the output signal and the amplitude ratio of output to input signal. These closed

loop responses were obtained for each set of values selected for the coefficients of the differential equation. The interrelationships of these coefficients with such parameters as system gain, damping ratio, and the undamped natural frequency will become apparent later in this report.

Plots of these experimental results were then correlated with theoretical curves obtained from calculations based upon the assumed functioning of the system components.

The investigation was carried out in the following stages:

(a) Theoretical analysis of the system based upon the assumed functioning of the various components;

(b) Determination of the range of linearity of each individual component of the system and thereby the establishment of the linear range of operation of the over-all system;

(c) Determination of the operating characteristics of the closed loop system and correlation with the theoretical results;

(d) Isolation and evaluation of any additional time delays unaccounted for in the original system design.

This investigation was conducted by the author at The Johns Hopkins University Applied Physics Laboratory, 8621 Georgia Avenue, Silver Spring, Maryland from July, 1951 until April, 1952.

2. THEORY

2.1 Basic Configuration.

The electromechanical analogue computing system is composed of the following basic components:

(a) Servo amplifier.

(b) Two-phase induction servo motor.

(c) Two-phase induction generator.

(d) Turntable or roll platform.

(e) Gear train and other connections.

These components are interconnected as indicated in Figure 1.

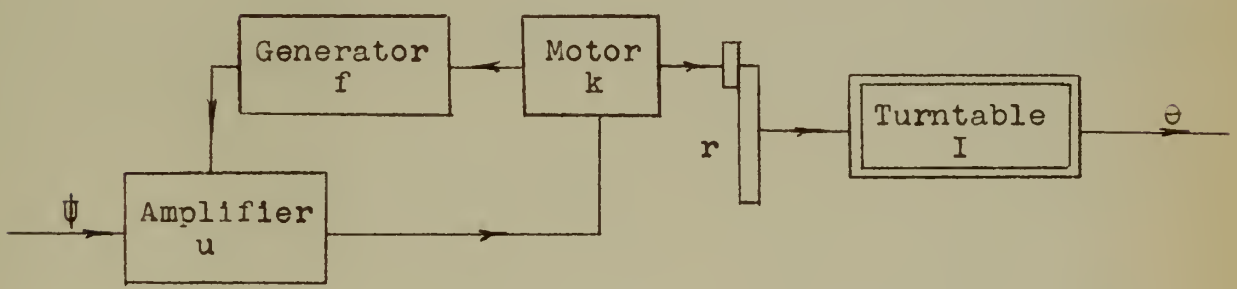

Fig. 1. Functional Diagram of the Computing System.

2.2 The Differential Equation to be Solved.

The differential equation to be solved can be expressed by

$$I\ddot{\theta} + G\dot{\theta} = -H\psi + T \qquad (2.2\text{-}1)$$

where θ = Angular displacement about the longitudinal or roll axis.

ψ = Angle of control surface from neutral position.

I = Inertia.

G = Coefficient of damping; i.e., due to wings.

H = Forcing function; i.e., roll torque per unit control surface angle.

T = Roll torque due to external causes.

Neglecting T and considering a perfect "proportional servo" control system;

$$\psi = K\theta \qquad (2.2\text{-}2)$$

where K is a constant, but adjustable, ratio of control surface displacement to roll angle.

The equation of motion now becomes

$$\ddot{\theta} + \frac{G}{I}\dot{\theta} + \frac{H}{I}k\theta = 0 \qquad (2.2\text{-}3)$$

or

$$\ddot{\theta} + a\dot{\theta} + b\theta = 0 \qquad (2.2\text{-}4)$$

where the coefficients a and b become measures of the damping and stiffness respectively.

2.3 Determination of the System Transfer Function by Dynamic Analysis.

A very brief functional description of the diagram in Figure 1 is as follows: The input signal (ψ) is generated by the movement of a control surface. It is then amplified ($u\psi$) and drives the induction motor. The motor torque ($uk\psi$) through an 18:1 gear ratio (n),

drives the turntable. The generator, mounted on the output shaft of the motor, is a damping device with an output proportional to the angular velocity of the turntable. Its output ($f\dot{\theta}$) provides negative feedback to the amplifier.

If there were no damping, the driving torque ($ukn\psi$) would equal the inertia retarding torque ($I\ddot{\theta}$) and the equation of motion would be

$$ukn\psi = I\ddot{\theta} \qquad (2.3\text{-}1)$$

where u is the amplifier gain, k is the motor gain, n is the gear ratio, ψ is the input signal, I is the inertia of the turntable and θ is the angular displacement of the table.

If now the damping effect of the generator is added, the equation of motion becomes

$$I\ddot{\theta} = ukn(\psi - f\dot{\theta}) \qquad (2.3\text{-}2)$$

Therefore,

$$I\ddot{\theta} + uknf\dot{\theta} = ukn\psi \qquad (2.3\text{-}3)$$

Dividing by I and simplifying gives

$$\ddot{\theta} + a\dot{\theta} = b\psi \qquad (2.3\text{-}4)$$

where $a = uknf/I$ and $b = ukn/I$. It is now apparent that if Equation 2.3-4 is to correspond to Equation 2.2-4

then the coefficients a and b are functions of the dynamic characteristics of the particular vehicle under test.

Employing the Laplace Transform (Ref. 4)[1] and indicating the Laplace operator by "s" gives

$$(s^2 + as)\,\theta(s) = b\psi(s) \qquad (2.3\text{-}5)$$

Thus,

$$\frac{\theta(s)}{\psi(s)} = \frac{b}{s^2 + as} = \frac{b}{s(s + a)} = \frac{b/a}{s(1/a\ s + 1)}$$

$$= \frac{K}{s(Ts + 1)} \qquad (2.3\text{-}6)$$

This is the open loop transfer function of the system when the computer is one component of a closed loop as in Figure 2.

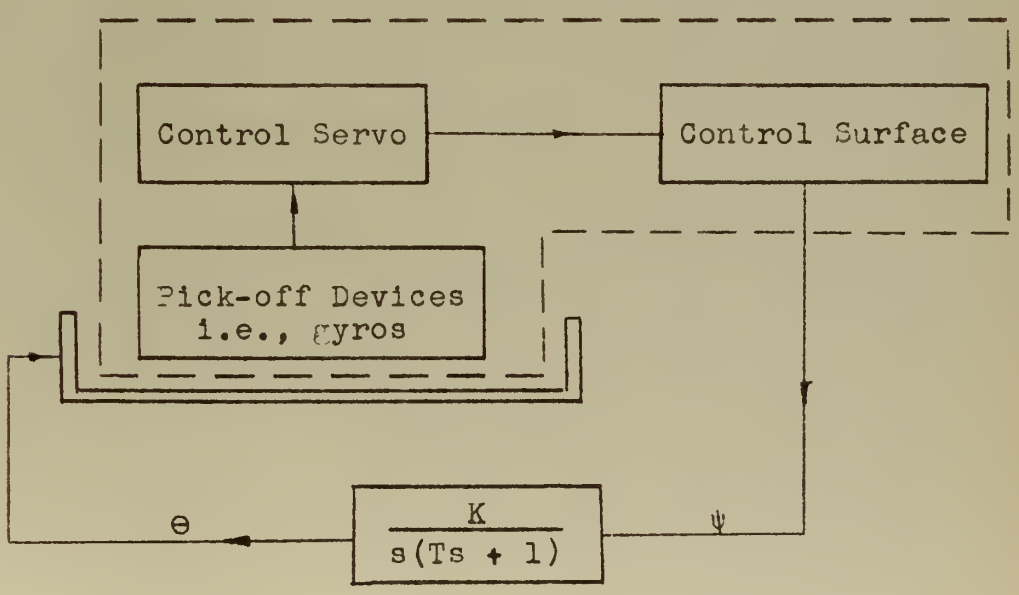

Fig. 2. Computer as one Component of a Closed Loop.

[1] References are listed in the bibliography of this report.

2.4 Determination of the Overall System Transfer Function by Servo Analysis.

The overall transfer function of the system can also be found by using block diagrams and the individual transfer functions.

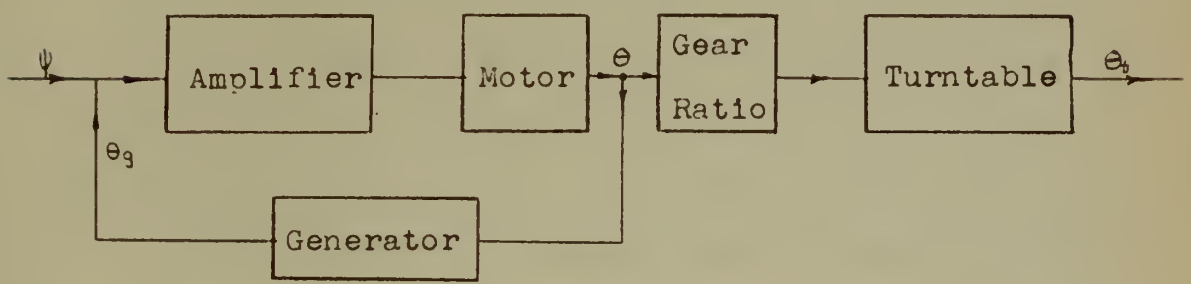

Fig. 3. Block Diagram of the Computer Components.

Figure 3 is a block diagram of the components. If there is assumed proper design of the gear ratio through rigid shafting, and thus no additional time lag in driving the turntable, the diagram can be simplified to that of Figure 4 without changing the form of the system transfer function.

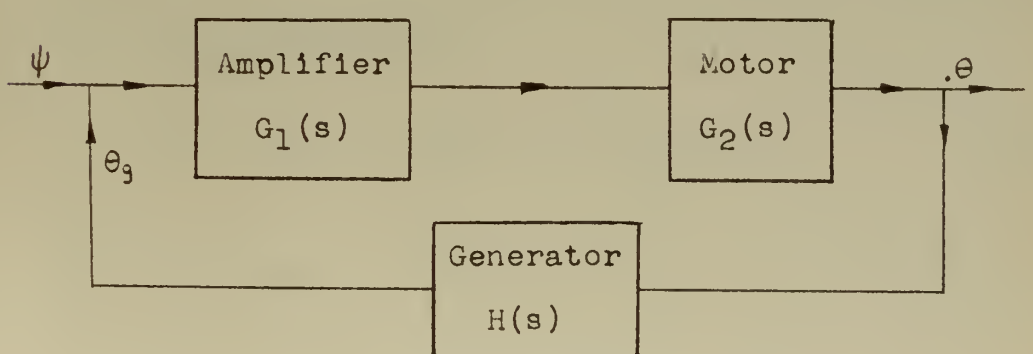

Fig. 4. Simplified Block Diagram.

It is now necessary to determine the individual transfer functions of the amplifier, the motor, and the generator.

Amplifier. The amplifier is assumed to be linear, within specified limits, with negligible time delay. Thus, its transfer function, $G_1(s)$, is simply K_a.

Motor. There has been much controversy over the form of the transfer function of a two-phase induction servo motor. The usual analysis (Ref. 1), based on steady state speed torque characteristics, results in a Laplace transfer function of the form

$$G_2(s) = \frac{K_m}{s(Ts + 1)} \qquad (2.4\text{-}1)$$

where, admittedly, the effect of the inductance and resistance of the windings has been neglected and the time constant is purely mechanical or a function of inertia and damping. Recently there have been indications (Ref. 5) that the transfer function might be more correctly expressed as

$$G_2(s) = \frac{K_m'}{s(T_1s + 1)(T_2s + 1)} \qquad (2.4\text{-}2)$$

where the second time constant may be considered an electrical delay equivalent to the ratio of inductance to resistance of the rotor. Initially it will be assumed

that Equation 2.4-1 is the correct expression for the motor transfer function.

Generator. Since the output of the generator is proportional to the angular velocity of the turntable,

$$\theta_g = K_g\dot{\theta} \tag{2.4-3}$$

or

$$\theta_g(s) = K_g s\theta(s) \tag{2.4-4}$$

Therefore, the feedback transfer function is

$$H(s) = \frac{\theta_g}{\theta}(s) = K_g s \tag{2.4-5}$$

Figure 4 can now be redrawn as shown in Figure 5.

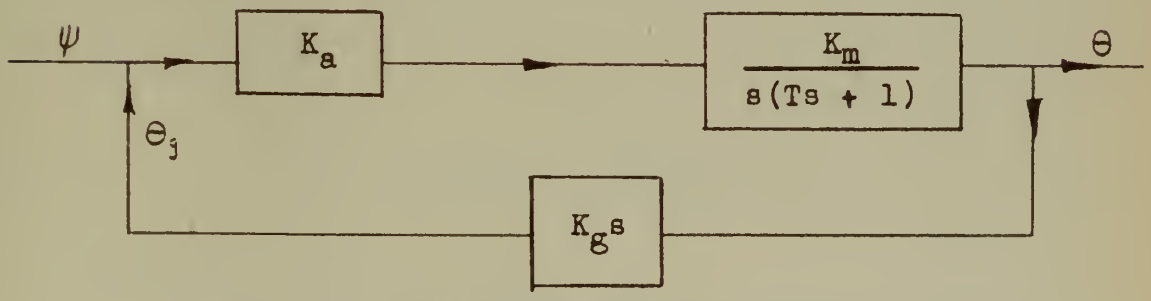

Fig. 5. Block Diagram with the Associated Transfer Functions of the Various Components.

From Figure 4 the overall system transfer function can be expressed as (Refs. 1,2, and 3)

$$G(s) = \frac{G_1(s)G_2(s)}{1 + G_1(s)G_2(s)H(s)} \tag{2.4-6}$$

Substituting for the individual transfer functions gives

$$G(s) = \frac{\dfrac{K_a K_m}{s(Ts + 1)}}{1 + \dfrac{K_a K_m K_g s}{s(Ts + 1)}} \qquad (2.4\text{-}7)$$

$$= \frac{K_a K_m}{s(Ts + 1) + K_a K_m K_g s} \qquad (2.4\text{-}8)$$

$$= \frac{K_a K_m}{s\left[Ts + (1 + K_a K_m K_g)\right]} \qquad (2.4\text{-}9)$$

or, finally,

$$G(s) = \frac{K'}{s(T's + 1)} \qquad (2.4\text{-}10)$$

This form of the overall system transfer function, determined by servo analysis, is the same as that determined by the dynamic analysis in Section 2.3.

If, however, the transfer function of the motor were actually

$$G_2(s) = \frac{K'_m}{s(T_1 s + 1)(T_2 s + 1)} \qquad (2.4\text{-}2)$$

then from Equation 2.4-5

$$G(s) = \frac{\dfrac{K_a K'_m}{s(T_1 s + 1)(T_2 s + 1)}}{1 + \dfrac{K_a K'_m K_g s}{s(T_1 s + 1)(T_2 s + 1)}} \qquad (2.4\text{-}11)$$

$$= \frac{K_a K'_m}{s(T_1 s + 1)(T_2 s + 1) + K_a K'_m K_g s} \qquad (2.4\text{-}12)$$

or

$$G(s) = \frac{K_a K_m'}{s\left[T_1 T_2 s^2 + (T_1 + T_2)s + (1 + K_a K_m' K_g)\right]} \qquad (2.4\text{-}13)$$

$$= \frac{K_a K_m'}{s(s + c)(s + d)} \qquad (2.4\text{-}14)$$

Where -c and -d are the roots of the quadratic.

Finally,

$$G(s) = \frac{K'}{s(T_1's + 1)(T_2's + 1)} \qquad (2.4\text{-}15)$$

2.5 Theoretical Development of the Expressions for the Amplitude Ratio and the Phase Shift for a Second Order System.

$$\text{If } G(s)_o = \frac{\theta(s)}{\Psi(s)} = \frac{K}{s(Ts + 1)} \qquad (2.3\text{-}6)$$

is the open loop transfer function of the system, then the closed loop transfer function can be expressed by (Ref. 1, page 141)

$$G(s) = \frac{G(s)_o}{1 + G(s)_o} \qquad (2.5\text{-}1)$$

Thus,

$$G(s) = \frac{\theta_o}{\theta_i}(s) = \frac{K/s(Ts + 1)}{1 + K/s(Ts + 1)} \qquad (2.5\text{-}2)$$

$$= \frac{K}{Ts + s + K} \qquad (2.5\text{-}3)$$

$$= \frac{1}{\frac{T}{K}s + \frac{1}{K}s + 1} \qquad (2.5\text{-}4)$$

If θ_i and θ_o, the input and output signals, are sinusoidally varying quantities, the Laplace operator "s" may be replaced by $j\omega$ (Ref. 1, page 96), where j is the complex operator and ω is the angular sinusoidal input variation.

Therefore,

$$G(j\omega) = \frac{1}{\frac{T}{K}(j\omega)^2 + \frac{1}{K}(j\omega) + 1} \qquad (2.5\text{-}5)$$

$$= \frac{1}{(1 - \omega^2 T/K) + j(\omega/K)} \qquad (2.5\text{-}6)$$

But

$$G(j\omega) = \frac{\theta_o}{\theta_i}(j\omega)$$

Therefore,

$$\left|\frac{\theta_o}{\theta_i}(j\omega)\right| = \frac{1}{\sqrt{(1 - \omega^2 T/K)^2 - (\omega/K)^2}} \qquad (2.5\text{-}7)$$

and if the phase between the output and input signal is ϕ, then

$$\phi = - \arctan\left[\frac{\omega/K}{1 - \omega^2 T/K}\right] \qquad (2.5\text{-}8)$$

$$= - \arctan\left[\frac{\omega}{K - \omega^2 T}\right] \qquad (2.5\text{-}9)$$

Where $K = b/a$, $T = 1/a$ and a and b are the constant coefficients of the equation of motion.

Equations 2.5-7 and 2.5-9 provide a means of theoretically predicting the amplitude ratio of output

to input signal and the phase angle by which the output lags the input.

2.6 The Interrelationships of the Constant Coefficients and the System Parameters of Damping Ratio and the Undamped Natural Frequency.

If the damping ratio, ζ, and the undamped natural frequency, ω_n, are to be expressed in terms of the constant coefficients a and b, the interrelationships existing among them must be determined.

From Section 2.2 the equation of motion is a second-order equation of the form

$$ID^2 + GD + Hk = 0 \qquad (2.6\text{-}1)$$

or

$$D^2 + aD + b = 0 \qquad (2.6\text{-}2)$$

where D is the operator for differentiation with respect to time. This equation has two roots R_1 and R_2:

$$R_1 \text{ and } R_2 = \frac{-G \pm \sqrt{G - 4IHk}}{2I} \qquad (2.6\text{-}3)$$

$$= \frac{-a \pm \sqrt{a - 4b}}{2}$$

For all stable systems, that is, those whose oscillations always attenuate to zero, the roots R_1 and R_2 may be (1) conjugate complex with negative real parts,

(2) equal negative real, or (3) unequal negative real, depending upon the numerical values of I, G, and Hk.

Two parameters, namely, the undamped natural frequency, ω_n, and the damping ratio, f, may be chosen so that the roots R_1 and R_2 may be expressed in terms of two quantities instead of three, as in Equation 2.6-3. One of these quantities, ω_n, has the dimensions of time; the other one, f, is dimensionless. Thus, if desired, a study of system behavior in dimensionless form can then be made.

The quantity ω_n is given by the characteristic Equation 2.6-1 when the damping is zero, that is,

$$ID^2 + Hk = 0 \qquad (2.6\text{-}4)$$

giving roots

$$R_1 \text{ and } R_2 = \pm j\sqrt{Hk/I} = \pm j\sqrt{b} = \pm j\omega_n \qquad (2.6\text{-}5)$$

therefore, $\omega_n = \sqrt{b}$. The parameter f or damping ratio is the ratio of actual damping to critical damping. Critical damping occurs when the radical of Equation 2.6-1 is zero or when the two roots R_1 and R_2 are equal. The critical value of damping, f_c, which can cause this condition is

$$f_c = 2\sqrt{HkI} \qquad (2.6\text{-}6)$$

The damping ratio is then

$$\zeta = \frac{\text{actual damping}}{f_c} = \frac{G}{2\sqrt{HkI}}$$

$$= \frac{a}{2\sqrt{b}} \qquad (2.6\text{-}7)$$

2.7 Calculated Results from the Expressions for the Amplitude Ratio and the Phase Shift Versus the Input Frequency.

It was desirable to be able to obtain the amplitude ratio, A, and the phase lag, ϕ, as functions of the input frequency in cycles per second, for each set of values given to the constant coefficients a and b.

A suitable range of representative values of a and b was then chosen. Values of a and b corresponding to damping ratios of 0.17, 0.3, 0.5 and 1.0 were selected and the phase and amplitude curves were calculated for angular frequencies ranging from 0.5 through 10.0 cycles per second.

The calculated phase-lag data are tabulated in Table I while the amplitude ratio data are recorded in Table II. These results are plotted in Figures 6 and 7; showing, respectively, the phase lag and amplitude ratio versus input angular frequency.

Table I. Calculated Phase-Lag Data for a Second Order System.

Frequency in cycles/second	Phase lag, ϕ, in degrees			
	$f = 0.17$	$f = 0.30$	$f = 0.50$	$f = 1.00$
0.2	----	----	----	11.4
0.5	5.2	9.1	14.9	28.1
1.0	12.7	21.8	33.7	53.0
1.5	30.1	45.8	59.6	-----
2.0	90.0	90.0	90.0	90.0
2.5	143.0	127.0	114.3	-----
3.0	157.8	144.2	130.1	112.7
4.0	167.2	158.1	146.2	126.8
5.0	170.9	164.1	154.4	136.5
7.0	174.0	169.5	162.8	148.2
10.0	176.0	172.9	168.3	157.4

Table II. Calculated Amplitude Ratio Data for a Second Order System.

Frequency in cycles/second	Amplitude ratio, A			
	$f = 0.17$	$f = 0.30$	$f = 0.50$	$f = 1.00$
0.5	1.060	1.050	1.040	0.944
1.0	1.300	1.240	1.110	0.803
1.5	1.970	1.550	1.150	0.641
2.0	-----	1.650	1.100	0.502
2.5	1.420	1.060	0.730	-----
3.0	0.740	0.650	0.510	0.309
4.0	0.340	0.310	0.280	0.201
5.0	0.190	0.180	0.170	0.138
6.0	-----	0.120	-----	0.100
7.0	0.090	0.087	0.084	0.075
9.0	-----	-----	-----	0.047
10.0	0.042	0.041	0.040	0.038
1.97*	2.980	-----	-----	-----
1.91*	-----	1.670	-----	-----
1.85*	-----	-----	1.170	-----

* Denotes the frequency at which the corresponding amplitude ratio is a maximum.

$$M_p = \frac{1}{2f\sqrt{1 - f^2}}$$ (Ref. 1, page 107)

Semi-Logarithmic, 3 Cycles X 6 to the ½ inch.
MADE IN U. S. A.

J. L. Miles
1st Lt. USMC

$\zeta = 1.7$

$\zeta = 3$

$\zeta = .5$

$\zeta = 1.0$

PHASE ANGLE, Φ (degrees)

12
24
36
48
60
72
84
96
108
120
132
144
156
168
180

Phase Lag vs Frequency
for
Closed Loop Second Order System

$$-\Phi = \arctan\left[\frac{\omega}{K-\omega^2 T}\right]$$

$$\zeta = \frac{a}{2\sqrt{b}}$$

Fig. 6

1 2 3 5 7 1.0 2 3 5 7 9

FREQUENCY (cycles per second)

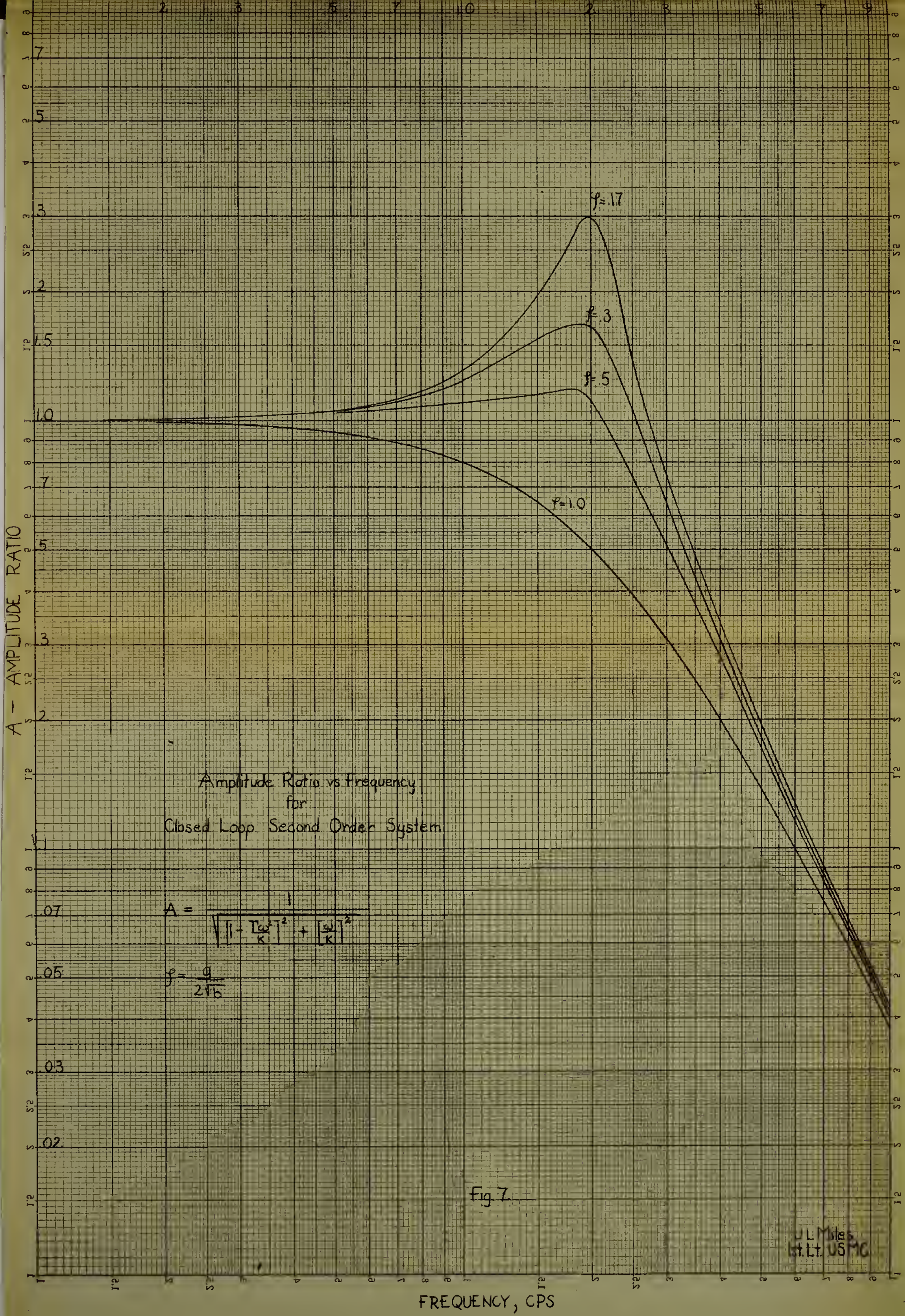
ζ=.17
ζ=.3
ζ=.5
ζ=1.0
A = 1 / √[(1 + Tω²/K)² + (ω/K)²]
ζ = a / 2√b
Amplitude Ratio vs Frequency
for
Closed Loop Second Order System
A - AMPLITUDE RATIO
FREQUENCY, CPS
.07
.05
.03
.02
J L Miles
1st Lt. USMC

Fig. 7

2.8 Development of Expressions for the Amplitude Ratio and Phase Shift for a Third Order System.

If the open loop transfer function for a third order system is given in the form of 2.4-15,

$$G(s)_o = \frac{K}{s(T_1 s + 1)(T_2 s + 1)} \qquad (2.8\text{-}1)$$

then the closed loop transfer function is given by

$$G(s) = \frac{\dfrac{K}{s(T_1 s + 1)(T_2 s + 1)}}{1 + \dfrac{K}{s(T_1 s + 1)(T_2 s + 1)}} \qquad (2.8\text{-}2)$$

$$= \frac{K}{s(T_1 s + 1)(T_2 s + 1) + K} \qquad (2.8\text{-}3)$$

$$= \frac{1}{\frac{T_1 T_2}{K} s^3 + \frac{T_1 + T_2}{K} s^2 + \frac{1}{K} s + 1} \qquad (2.8\text{-}4)$$

If the input signal is sinusoidal, "s" can be replaced by $j\omega$ and the equation becomes

$$G(j\omega) = \frac{1}{\frac{T_1 T_2}{K}(j\omega)^3 + \frac{T_1 + T_2}{K}(j\omega)^2 + \frac{j\omega}{K} + 1} \qquad (2.8\text{-}5)$$

$$= \frac{1}{\left[1 - \omega^2/K(T_1+T_2)\right] + j\left[\omega/K - \omega^3/K(T_1 T_2)\right]} \qquad (2.8\text{-}6)$$

and

$$G(j\omega) = \frac{\theta_o}{\theta_i}(j\omega)$$

Therefore,

$$\frac{\theta_o}{\theta_1}(j\omega) = \frac{1}{\sqrt{\left[1 - \frac{\omega^2}{K}(T_1+T_2)\right]^2 + \left[\frac{\omega}{K} - \frac{\omega^3}{K}(T_1T_2)\right]^2}} \qquad (2.8\text{-}7)$$

The phase angle between output and input signals is then

$$\phi = - \arctan \frac{\omega - \omega^3 T_1 T_2}{K - \omega^2(T_1+T_2)} \qquad (2.8\text{-}8)$$

3. EXPERIMENTAL PROCEDURE AND RESULTS.

3.1 Description of Components.

3.1-a The Power Amplifier.

A schematic of the amplifier and power supply is shown in Figure 8. The components are built into the body of the computer with the exception of the mixing circuit which is contained in the externally mounted case shown in Figure 11.

The mixing circuit is a conventional two-channel mixer which adds the output of the turntable, from a #1 Control Transformer, to the negative feedback of the generator; the algebraic sum feeding into the inverter network.

The phase inverter receives a single-ended input and derives voltages for the push-pull grids that are 180 degrees out of phase over the complete frequency range of the amplifier.

The output tubes are in push-pull to obtain increased power with less distortion; the even harmonics cancel. The power out is proportional to the number of tubes used. Thus, eight 6L6's are used to give sufficient output power.

This unit was designed and constructed at the Applied Physics Laboratory.

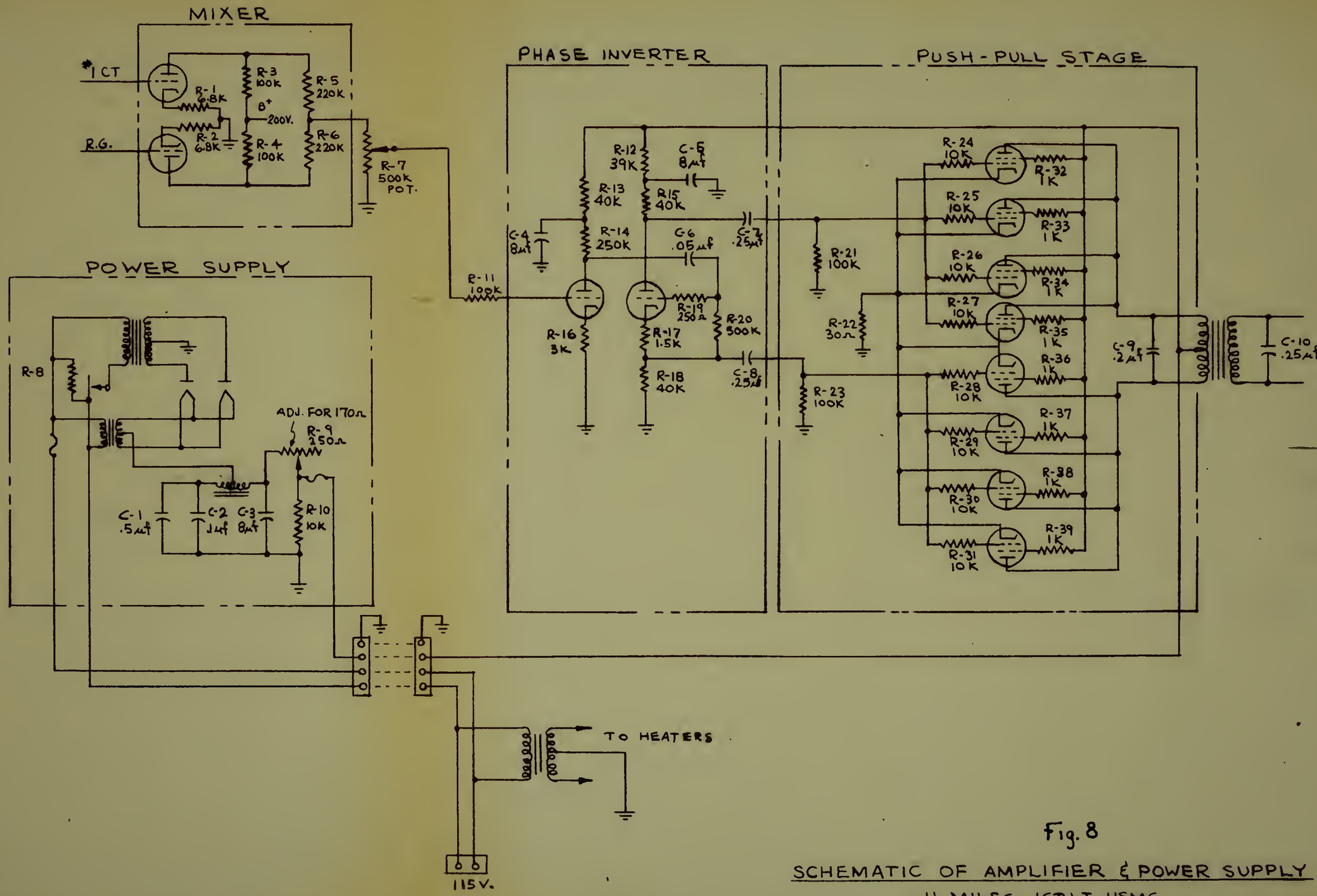

Fig. 8

SCHEMATIC OF AMPLIFIER & POWER SUPPLY

J.L.MILES 1ST.LT. USMC

3.1-b The Motor.

An Arma #6 Induction Motor (Reference 6) is a two-phase two-pole motor having a thin shell cup rotor and a stationary core, and is designed to operate on 60 cycle alternating current. There are two field windings which are in space quadrature: one the main field, and the other the control field. A constant 60 cycle voltage of 115 volts is applied to the main field and a variable 60 cycle voltage, which is in phase quadrature to the main field voltage, is applied to the control field. Reversal of rotation is is accomplished by reversal of direction of the voltage applied to the control field.

The applied voltages are rarely balanced, for to achieve control of torque and direction of rotation, the control-winding voltage may be varied from rated value in one sense through zero to rated value in the opposite sense while the voltage on the other winding is held constant.

When it is necessary to have a fast acting yet stable closed-cycle control system, it is highly desirable that the torque-to-inertia ratio of the servomotor have a large value. For this reason the rotor consists only of a thin hollow cup of light conducting material in order to reduce inertia. The magnetic path is completed by means of a stationary cylinder of

iron placed inside the rotor. There are thus two clearance air gaps. Motors made in this manner are frequently called "drag cup" motors.

This type of construction means that the exciting current as compared with that of motors of conventional design, is relatively large. Closed-cycle control systems normally require a servomotor with characteristics typical of high-rotor resistance. High-rotor resistance may combine with high exciting current to produce comditions which prevent the motor from developing any running torque when operating single phase regardless of speed. This is a very desirable characteristic for many control applications although it is an intolerable condition in split-phase or capacitor motors.

The dimensions of the Arma #6 Motor are given in Figure 9 while its relative size and location within the computer system is photographed in Figure 11.

3.1-c The Feedback Generator.

In servomechanisms and electromechanical computing systems it is often necessary to generate an A. C. voltage which is proportional to the speed of an input shaft. The ideal machine for such applications is one which generates a voltage proportional to the rotor speed without the introduction of phase shift,

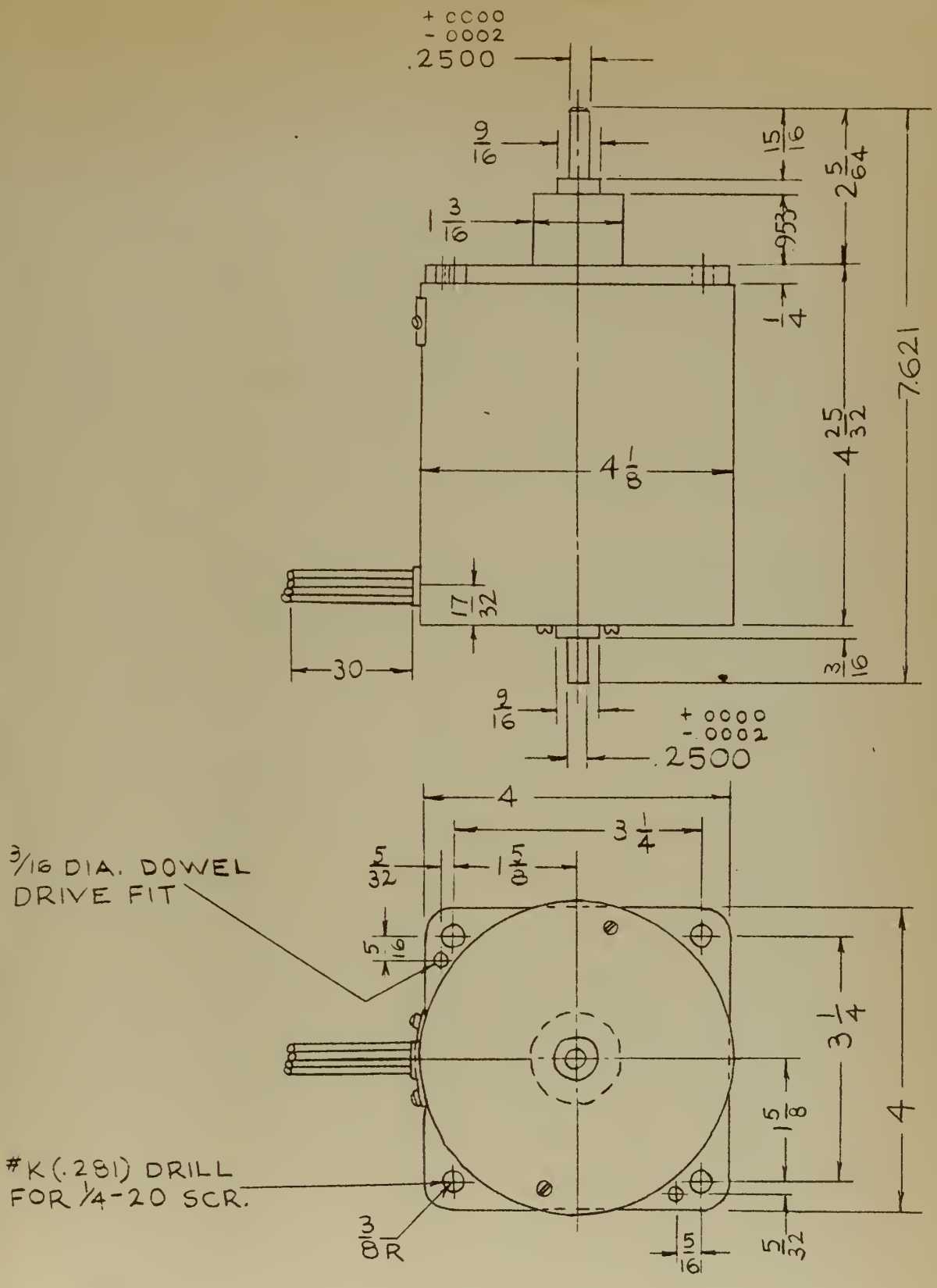

The Arma 6 Induction Motor

Fig. 9

harmonics or quadrature voltage. It should also be small in size, require little excitation power, have low inertia and a minimum of friction.

Such a device is the Arma #3 Induction Generator having a stationary core and a thin shell cup rotor. There are two fields, main and control, whose axes are in space quadrature. A voltage is induced in the control field proportional to the speed of the cup.

The generator dimensions are given in Figure 10 while relative size and location are photographed in Figure 11.

3.1-d The Assembled Computer.

The entire system is housed in a device about 40 inches wide and 36 inches high. It is portable and completely self contained (less recorders). Figure 11 is a photograph of the computer. Since no pick-off devices were mounted during the analysis, the turntable has been replaced by a rotating shaft which drives the arm of the recording potentiometer. The control panel contains dials for setting the "damping" and "stiffness" of the system. The use of these and the various other dials and switches will become evident as the calibration procedure is described.

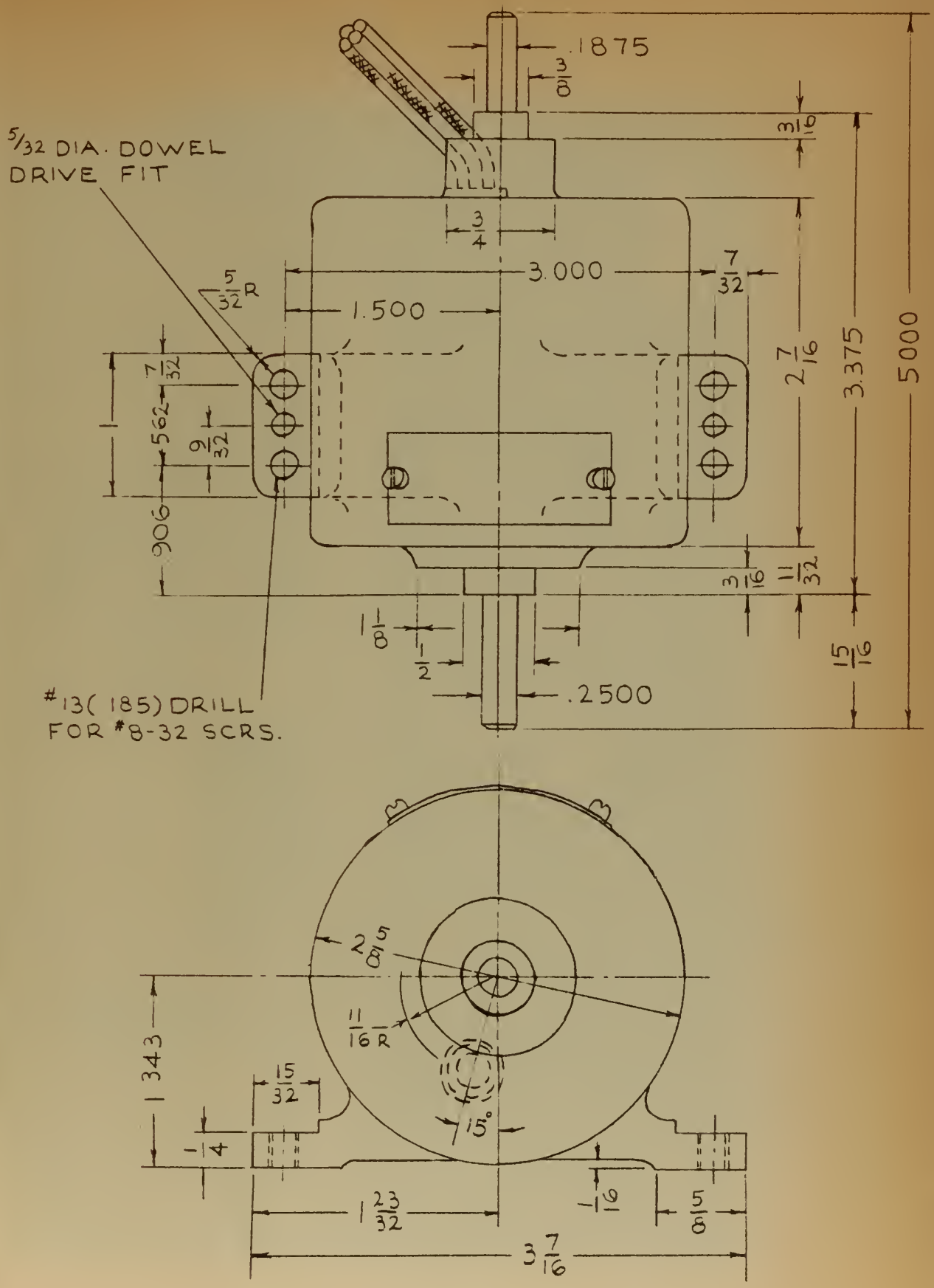

The Arma 3 Induction Generator

Fig. 10

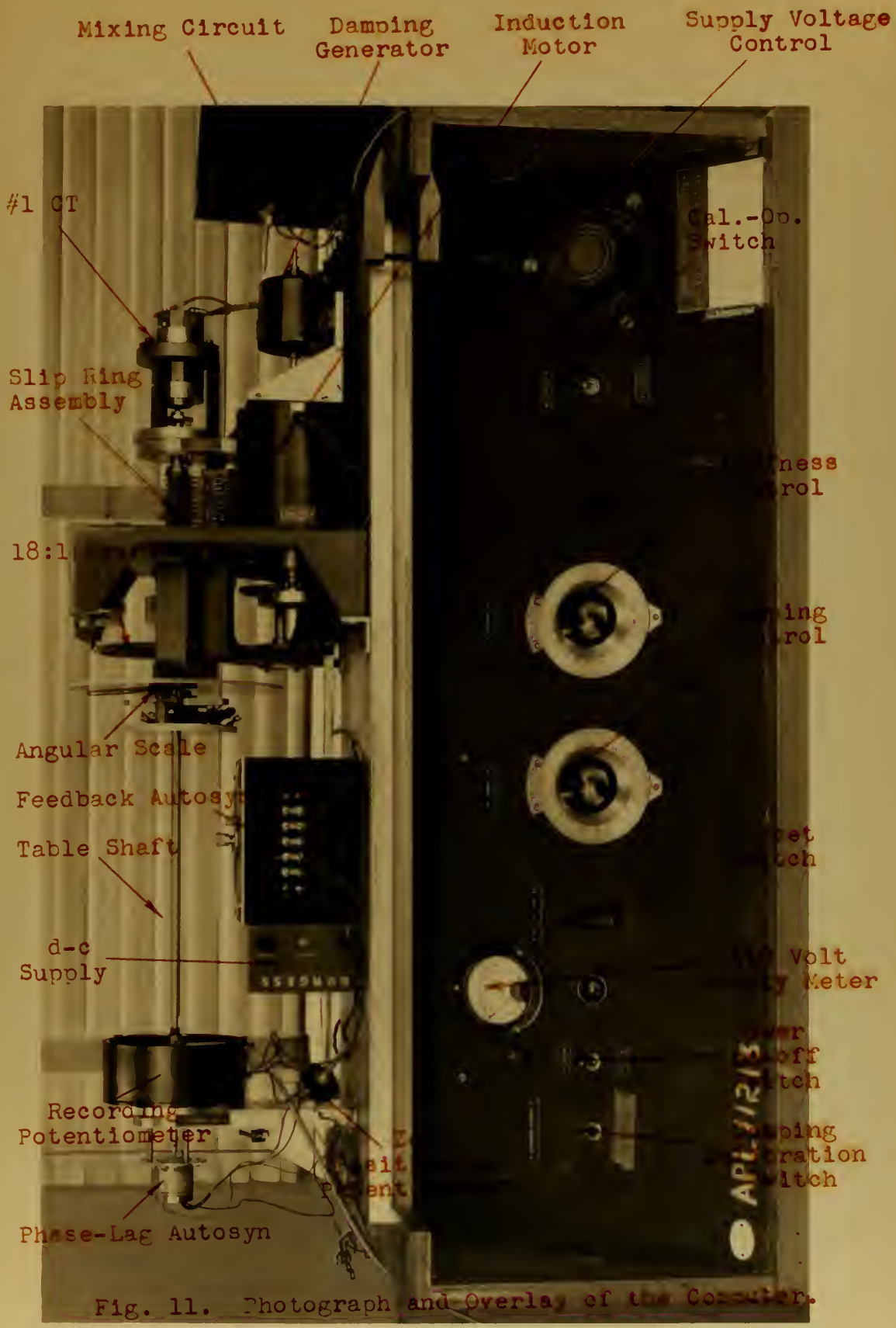

Fig. 11. Photograph and Overlay of the Computer.

THE JOH[illegible] UNIVERSITY
THE PHOTOGRAPH DUPLICATING
8621 GEORGIA AVENUE
PHOTO NUMBER
888
DATE PRINTED

3.2 Computer Calibration and Operation.

Perhaps better understanding of the operating principles of the computer can be obtained by means of a typical illustration.

Figure 12 is an amplified version of Figure 2 and shows a closed loop system composed of the computer and a test servo. The test servo is only an example and could be of many configurations to perform one of several functions. Possible uses are, for example; the simulation of a control system to stabilize a gun platform aboard ship or plane, roll stabilization of a guided bomb or rocket, and even the roll stabilization of a submarine, although in actuality other methods are employed.

Perhaps one of the paramount advantages of this system should be emphasized here. The presence of the turntable or roll platform, upon which the actual sensing devices of a test servo-loop may be mounted, is of extreme importance. This allows exact duplication and minimizes the amount of analytical simulation necessary. If it is desirable to study the effects of external disturbance torques on a particular test vehicle, the gyroscopes from the vehicle can be mounted on the turntable and the disturbance torque introduced into the system by merely tilting the table

DATE PRINTED

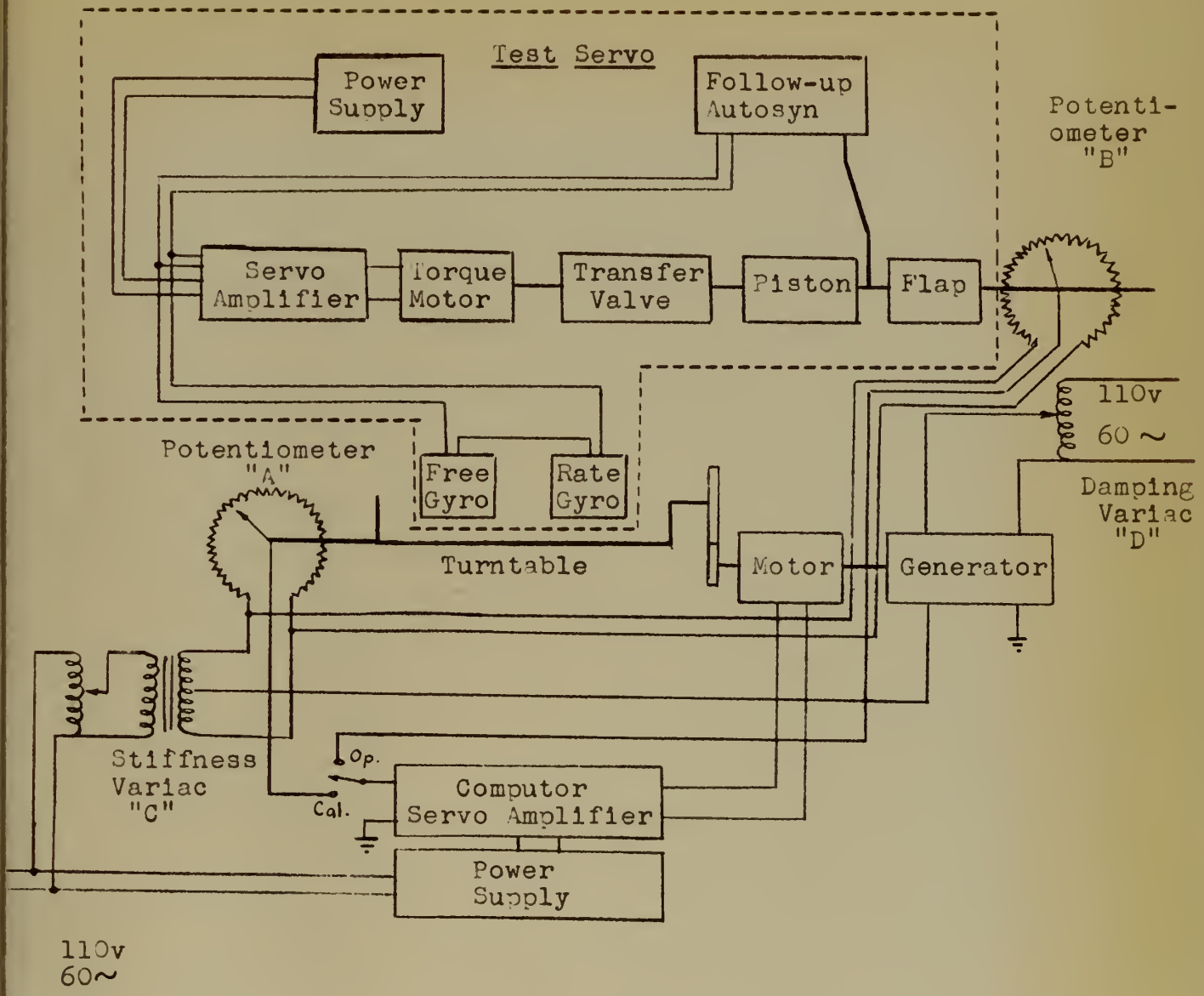

Figure 12. Computer and Test Servo Loop.

and suddenly releasing it. In this manner the computer can be used to study the response, in roll, to any external disturbance by introducing a deflection as a step function.

Returning to Figure 12, the turntable carries

a free gyro and a rate gyro. An autosyn on the free gyro delivers a signal voltage proportional to the angle of rotation (θ) of the table; and the rate gyro, through a pick-off, supplies a voltage in series with the former but of opposite phase, for damping purposes.

Upon deflecting the platform from its neutral position, a signal proportional to the roll angle (θ) is fed into the test servo; which, by means of its hydraulic piston, turns the flap through the angle ψ. A potentiometer operated by this flap establishes a signal voltage proportional to ψ. This voltage is fed to the computer amplifier, the output of which powers the servo motor which in turn drives the turntable and causes it to return to its original position. The system thus is a computer designed to solve the dynamic equation. Damping of the computer servo is effected by the Arma generator on the shaft of the motor, its output being in series with the amplifier input.

To set up the computer for operation, it is first necessary to introduce values of a and b as determined from dynamic studies of the test vehicle being used. This process calibrates the system for operation.

With the "calibrate-operate" switch in the "calibrate" position (disconnecting the test servo), the damping coefficient, a, is made zero (or practically

so) by turning the computer damping control to zero (adjusting Variac D). Equation 2.2-4 then becomes

$$\ddot{\theta} + b\theta = 0 \qquad (3.2\text{-}1)$$

from which the undamped natural frequency was found to be $\sqrt{b}$ (Section 2.6), or

$$F_n = \sqrt{b}/2\pi \text{ cycles per second.} \qquad (3.2\text{-}2)$$

If then, with the damping control set at zero, the turntable is displaced and allowed to oscillate, its slightly damped frequency will be practically equal to the undamped frequency given by Equation 3.2-2. To calibrate, therefore, it is merely necessary to adjust the stiffness control (Variac C) until the frequency of oscillation, as measured on a Brush recorder, is equal to the value given by Equation 3.2-2. More specifically, a potentiometer, whose arm is driven by the turntable shaft, is connected to a Brush magnetic oscillograph which provides an amplitude versus time trace from which the "natural" frequency of the computer loop may be determined. The voltage across potentiometer A, driven by the turntable, is adjusted by means of Variac C. This adjustment varies the voltage fed into the amplifier for a given angular displacement of the table; and hence, in effect, changes the stiffness factor, b, of the system.

To calibrate the damping, or set in the correct value of a, a steady-state roll of the turntable must be produced. To do so, the computer servo loop must be broken and a signal introduced corresponding to a constant flap displacement, ψ. This constant signal causes the drive motor to run at a constant speed.

It is apparent from Equation 2.3-4

$$\ddot{\theta} + a\dot{\theta} = b\psi$$

that if ψ is given some fixed displacement, ψ_o (say 5°), the system rapidly acquires a steady roll velocity, whose magnitude is given by

$$\dot{\theta} = b\psi_o/a \quad \text{radians per second.} \qquad (3.2\text{-}3)$$

Since b is known and has been set in, and since ψ_o is a known constant quantity, it is a simple matter to compute the value of velocity which will occur when the desired value of a is substituted in Equation 3.2-3. The damping calibration procedure, therefore, is to adjust the damping of the system, by means of the damping control (Variac D), to obtain a Brush recording indicating the required value of $\dot{\theta}$. This procedure inserts the required damping factor, a, into the system. It should be noted that Equation 3.2-3 gives the velocity in radians per second and not in revolutions per second. In order to supply a constant angle of ψ_o to the system,

the computer has a displacement signal switch (Fig. 11); which, when turned to either the left or the right position, applies an effective constant flap displacement of 5 degrees to the system. Thus, the value of ψ_o to use in Equation 3.2-3 is $5\pi/180$. When the above steps have been carried through, the computer is theoretically calibrated and ready for use.

In the interest of learning more about the device, a method for checking the accuracy of calibration will now be discussed. To do this, a recording of the damped oscillation or "transient response curve" following an initial displacement of the turntable may be compared with the corresponding theoretical "transient response curve" calculated from Equation 2.2-4. The solution of this equation is derived in the appendix and is given by

$$\theta = \frac{\theta_o}{\cos} e^{-at/2} \cos(\omega t - \beta) \qquad (3.2\text{-}4)$$

where $\omega = \sqrt{b - (a/2)^2}$

β = arctan a/2

θ_o = initial displacement of table in radians.

Having now a theoretical expression for the response, it is possible to experimentally measure the response by displacing the turntable, releasing it, and recording the motion by means of a Brush recording

oscillograph. Comparison of the two curves will give an indication of the accuracy of calibration.

In plotting the response curves, it is not necessary to plot whole curves, but merely the exponential envelope. If Equation 3.2-4 is examined, it will be seen that whenever $|\cos(\omega t-\beta)| = 1$, θ falls on the curve

$$\frac{\theta_o}{\cos\beta} e^{-at/2}$$

which is the equation of the envelope. These points occur in time whenever $(\omega t - \beta) = n\pi$, or $t = (n\pi-\beta)/\omega$, where n = 0,1,2,3,---etc. It will then be necessary, for the present purpose, to plot only those values of θ which occur when t has the above values. Experimentally, these points correspond to values of t occurring mid-way between successive intercepts on the time axis, or the peak values.

Further simplification results when it is noticed that, assuming $|\cos(\omega t - \beta)| = 1$ (which is true at the points in question), the logarithm of θ is a linear function of time. Thus, if the response curves are plotted, as mentioned above, on semi-log paper, with θ along the log axis and time along the linear axis, the curves should be straight lines. Therefore, when the peak values of the recorded transient response curve of the computer are plotted

on the same graph sheet with the straight "exponential decay" line, a direct comparison between the theoretical and the actual transient responses can be obtained.

Figure 13 is a series of calibration traces for various values of a and b. The corresponding accuracy check-plots are shown in Figure 14 with the solid lines representing the calculated exponential decay, while the plotted points represent the magnitudes of the recorded peak values.

A study of Figure 14 indicates that the computer was accurately calibrated for these particular values. It will be noted that the experimental values begin to "fall off" when the peak amplitudes become small or the transient has nearly died away. It is believed that this non-linear effect is due to friction and is not appreciable until the amplitude of oscillation has decreased to less than one-third of the initial displacement.

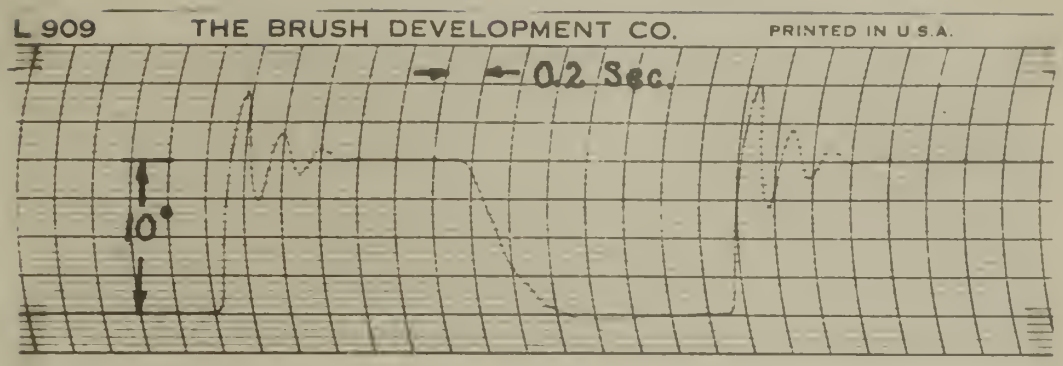

Fig. 13-a. a = 9.6 and b = 800

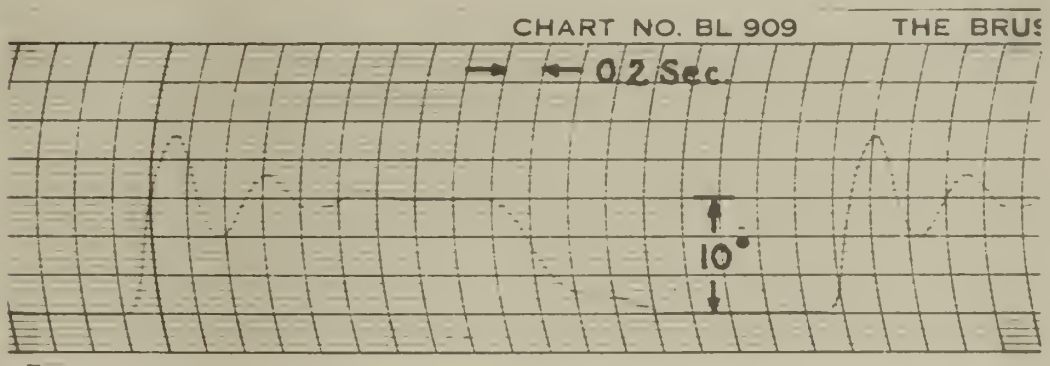

Fig. 13-b. a = 4.27 and b = 158

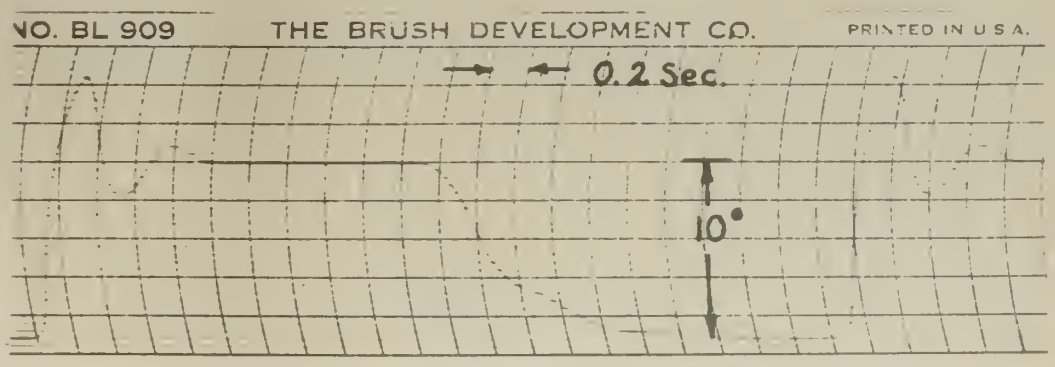

Fig. 13-c. a = 7.56 and b = 158

Fig. 13. Calibration Traces for Various Values of a and b.

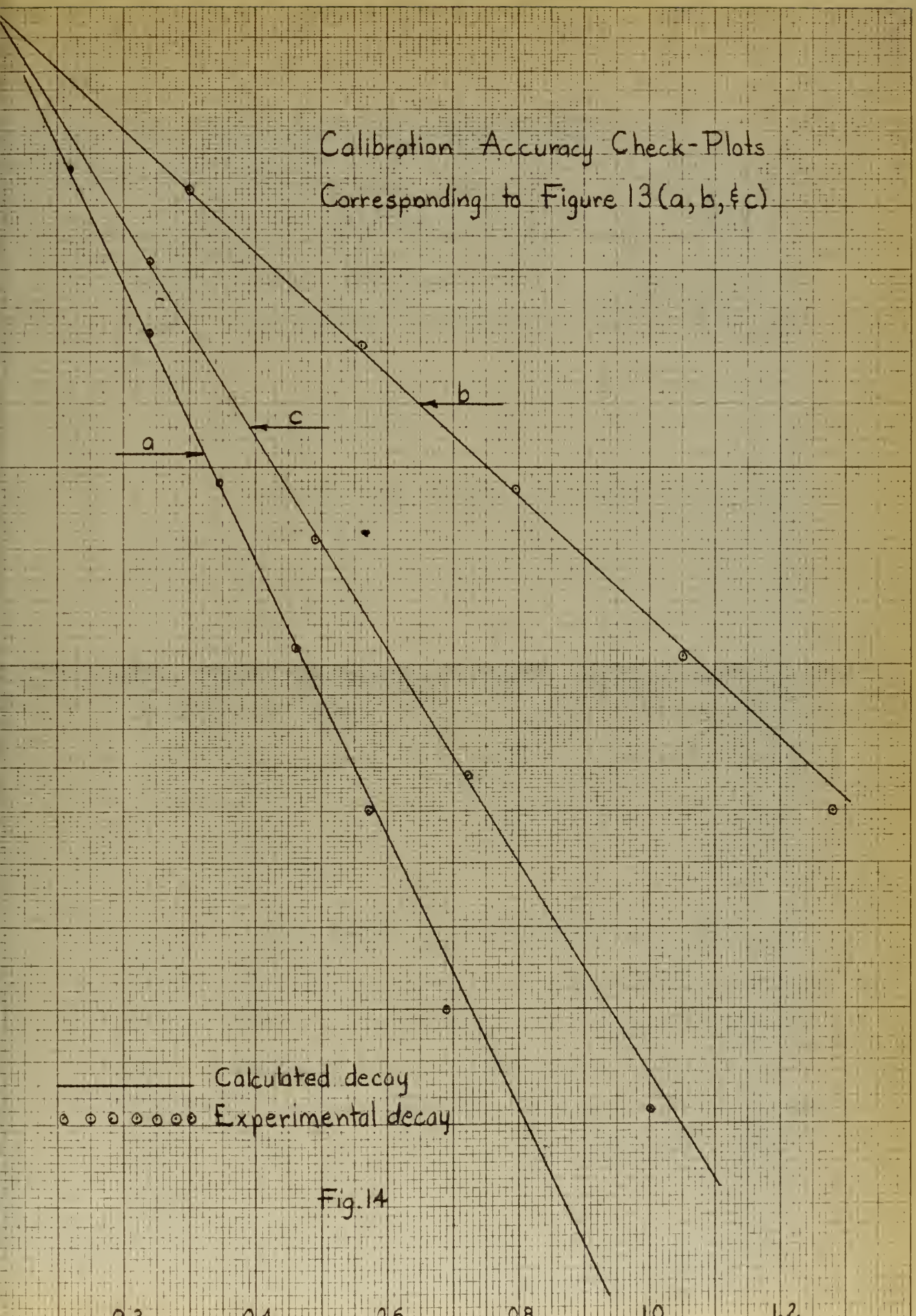
Calibration Accuracy Check-Plots
Corresponding to Figure 13 (a, b, & c)
a
c
b
Calculated decay
Experimental decay
0.2
0.4
0.6
0.8
1.0
1.2
Time in Seconds

Fig. 14

3.3 Establishing the Linear Limits.

The following sequence of investigations was conducted to establish the linear limits of the various components and thus insure that all subsequent operations were performed within the linear range of the system.

3.3-a Amplifier.

To verify the assumption that the amplifier is a linear component, the output and input voltages were recorded as functions of the angle of roll of the turntable. These data are tabulated in Table III. The results are clearly shown in Figure 15 and indicate linearity of amplifier output up to 11 or 12 degrees of table roll. Consequently, the roll angle of the table was hereafter confined to this maximum.

3.3-b Motor.

From typical motor performance curves for the Arma #6 Induction Motor, the stall torque is found to be directly proportional to the control field voltage. A graph of this relationship is taken from Reference 6 and reproduced in Figure 16. This property also has been verified at the Applied Physics Laboratory.

Table III. Amplifier Input and Output vs. Turntable Roll Angle.

Roll Angle	Input Voltage	Output Voltage
1	0.030	8.0
2	0.057	17.0
3	0.084	25.0
4	0.105	33.0
5	0.132	40.0
6	0.158	49.0
7	0.184	57.0
8	0.210	65.0
9	0.235	72.0
10	0.260	80.0
11	0.288	88.0
12	0.310	95.0
13	0.335	102.0
14	0.360	106.0
15	0.385	-----

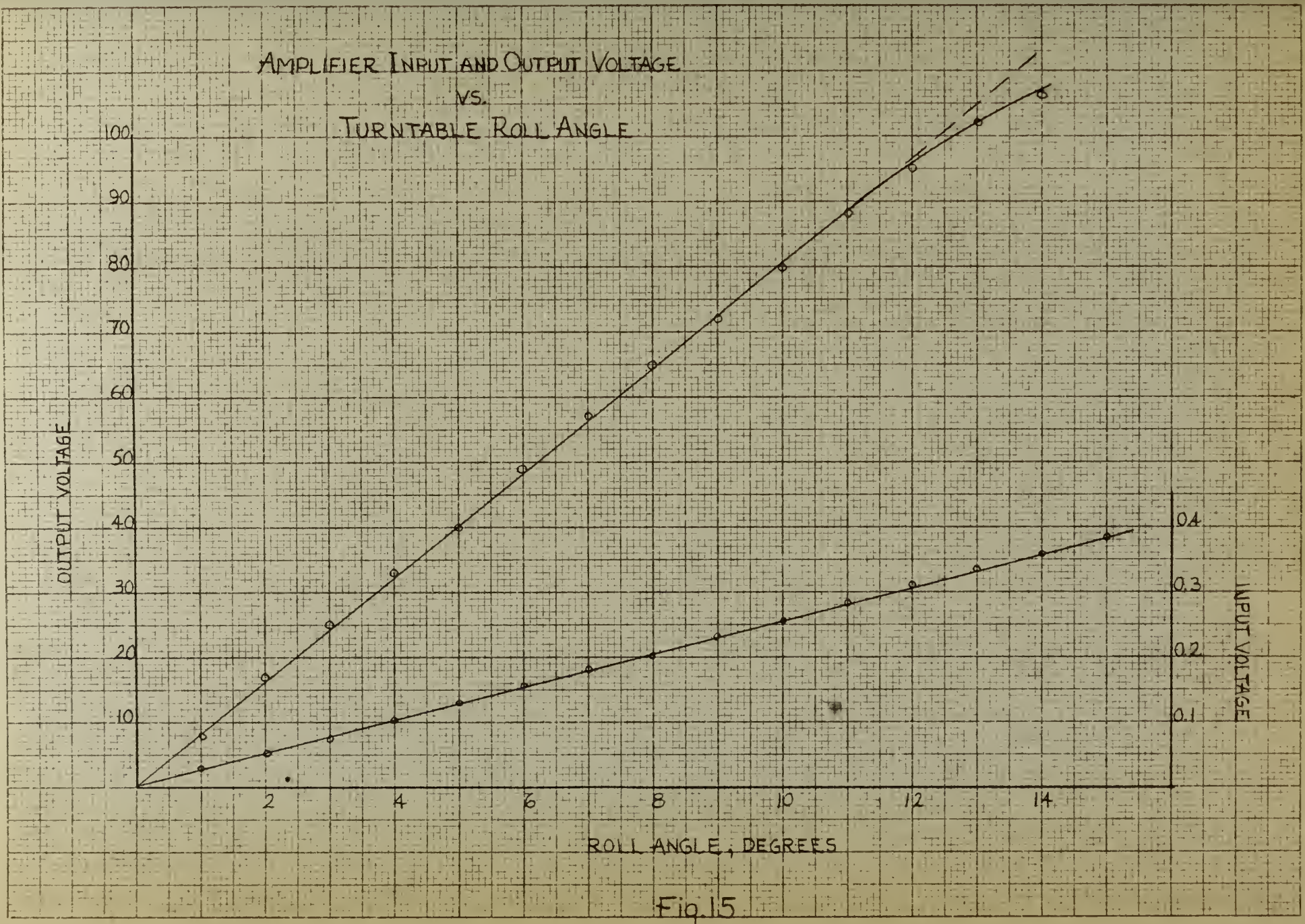
AMPLIFIER INPUT AND OUTPUT VOLTAGE
VS.
TURNTABLE ROLL ANGLE
OUTPUT VOLTAGE
100
90
80
70
60
50
40
30
20
10
INPUT VOLTAGE
0.4
0.3
0.2
0.1
2
4
6
8
10
12
14
ROLL ANGLE, DEGREES

Fig. 15

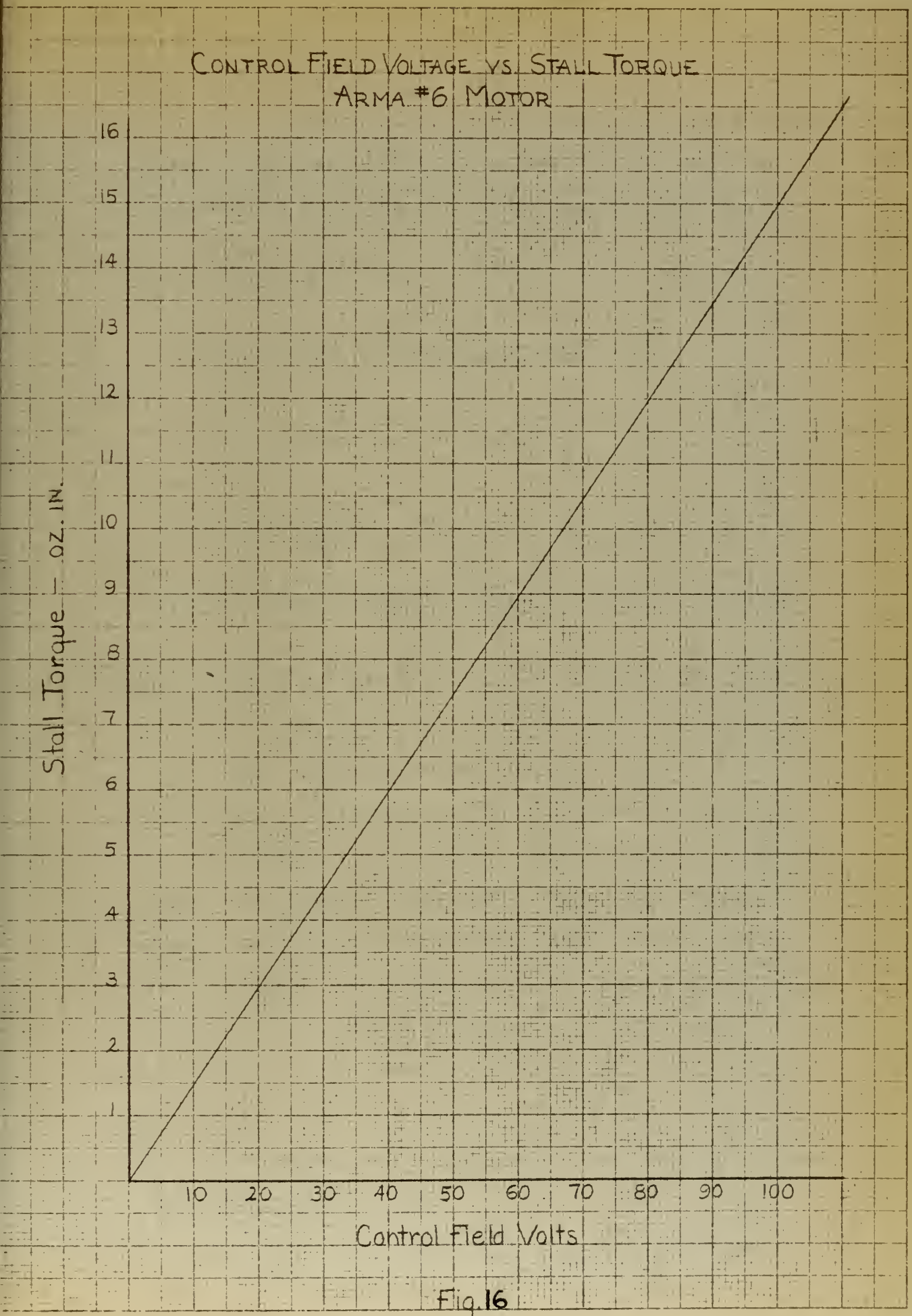
CONTROL FIELD VOLTAGE VS. STALL TORQUE
ARMA #6 MOTOR
Stall Torque - oz. in.
16
15
14
13
12
11
10
9
8
7
6
5
4
3
2
1
10
20
30
40
50
60
70
80
90
100
Control Field Volts

Fig. 16

If the speed-voltage-torque characteristics of the motor were ideal, they would be of the form illustrated in Figure 17. The torque would then be

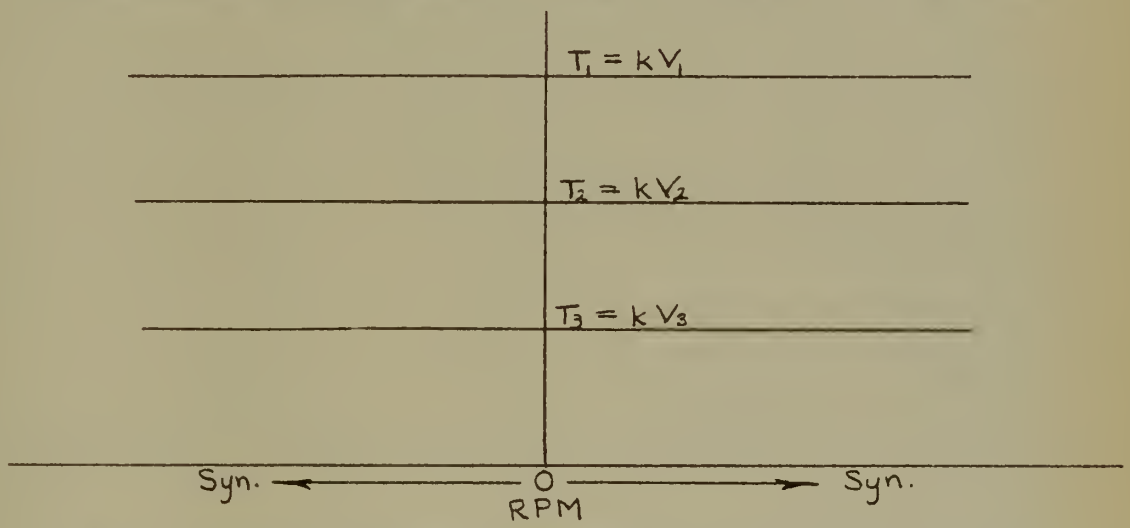

Fig. 17 Ideal Speed-Voltage-Torque Relationships for the Motor

proportional to the control field voltage but independent of speed. Therefore, it is necessary to investigate the speed-torque relation of this motor. This has been done extensively in Reference 9 for the Arma #6 motor in a similar circuit. The actual speed-torque relation was found to be that of Figure 18. Thus, the torque is seen to be comparatively independent of speed at low velocities and becomes more and more a function of speed as the velocity increases. If the speed is limited to one-half synchronous speed (1600 rpm) in either direction, the torque produced is nearly a constant. The following analysis will reveal the limiting effect of restraining the speed.

Fig. 18

Speed - Torque Curves
ARMA #6 MOTOR

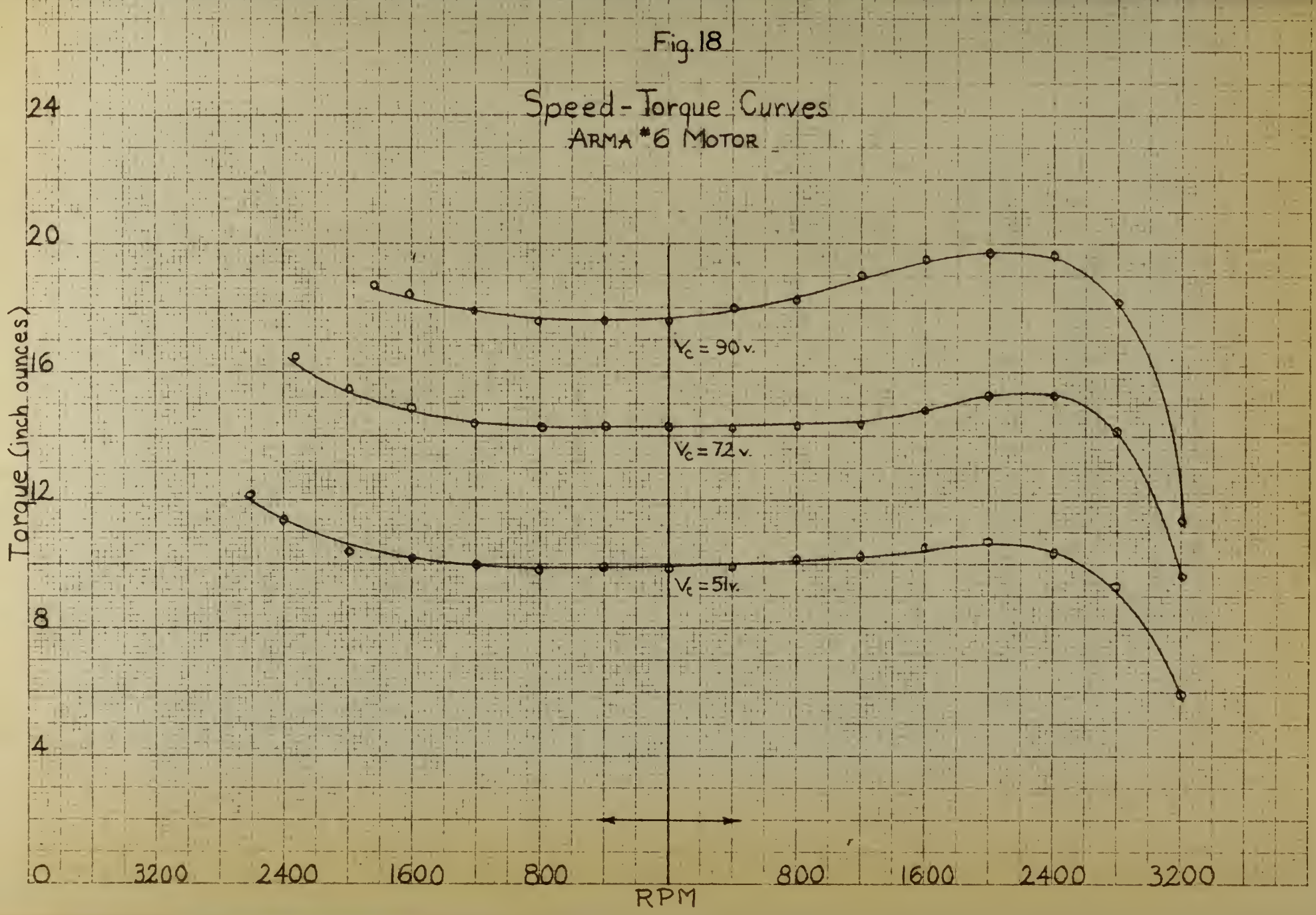

Converting the speed in revolutions per minute to degrees per second results in

$$\frac{1600\text{rpm} \times 360\text{deg/rev}}{60\text{sec/min} \times 18} = 533 \text{ deg/sec} \qquad (3.3\text{-}1)$$

where 18:1 is the gear ratio between motor and turntable.

The maximum angular displacement of the turntable occurs at the resonant frequency which is approximately two cycles per second for the theoretical curves of Figure 7.

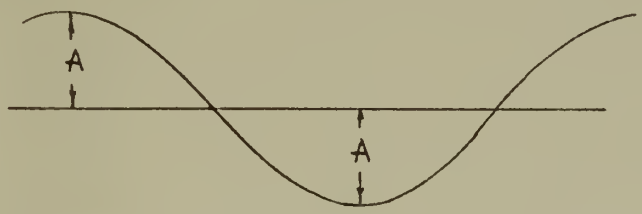

From the sine wave above, it is apparent that the maximum velocity is equal to the peak amplitude multiplied by the angular velocity, or

$$\text{Amplitude} = A = \frac{\dot{\theta}}{\omega} = \frac{533}{2\pi f} = \frac{533}{4\pi} \qquad (3.3\text{-}2)$$

$$= 42.5 \text{ degrees}$$

Obviously, other factors of linearity will limit the value of table rotation below this value. Thus, limiting the speed of the motor to one-half synchronous speed will still permit sufficient angular displacement of the turntable.

3.3-c Generator.

The assumption having been made that the output voltage was proportional to the input shaft rate, it was necessary to verify the linearity of output voltage versus turntable velocity for the generator. This was done by recording the table velocity, in cycles per second, on a Brush Recorder while reading the corresponding output voltage of the generator. This was done for a range of damping ratios from 0.1 to 1.0. The data are tabulated in Table IV; while the velocity, converted to degrees per second, is plotted versus the output voltage in Figure 19.

These results establish the linear relation between generator feedback voltage and the roll velocity of the table.

3.3-d Recording Potentiometer.

The linearity of the recording potentiometer was also verified by measuring the output signal voltages corresponding to various angles of roll of the table.

These data are recorded in Table V and plotted in Figure 20.

All subsequent utilization of the system was conducted within the linear range of operation as established herein.

Table IV. Generator Output Voltage vs. Turntable Angular Velocity.

$f = 1.0$

Volts	cps	deg/sec
0.100	0.105	38.0
0.190	0.233	84.0
0.300	0.375	135.0
0.395	0.490	176.0
0.495	0.620	223.0
0.600	0.750	270.0
0.695	0.875	315.0
0.795	0.995	358.0
0.895	1.143	412.0
0.995	1.250	450.0
1.090	1.375	495.0
1.200	1.500	540.0

$f = 0.5$

Volts	cps	deg/sec
0.218	0.110	78.0
0.357	0.195	130.0
0.532	0.285	192.0
0.667	0.355	240.0
0.800	0.425	288.0
1.020	0.545	368.0
1.286	0.675	464.0
1.470	0.770	529.0
1.670	0.870	600.0

$f = 0.3$

Volts	cps	deg/sec
0.050	0.137	49.0
0.100	0.300	108.0
0.200	0.625	225.0
0.295	0.935	337.0
0.395	1.250	450.0
0.495	1.600	576.0
0.600	1.930	694.0

$f = 0.1$

Volts	cps	deg/sec
0.050	0.400	144.0
0.075	0.625	225.0
0.100	0.855	308.0
0.125	1.110	400.0
0.150	1.330	478.0
0.180	1.600	575.0

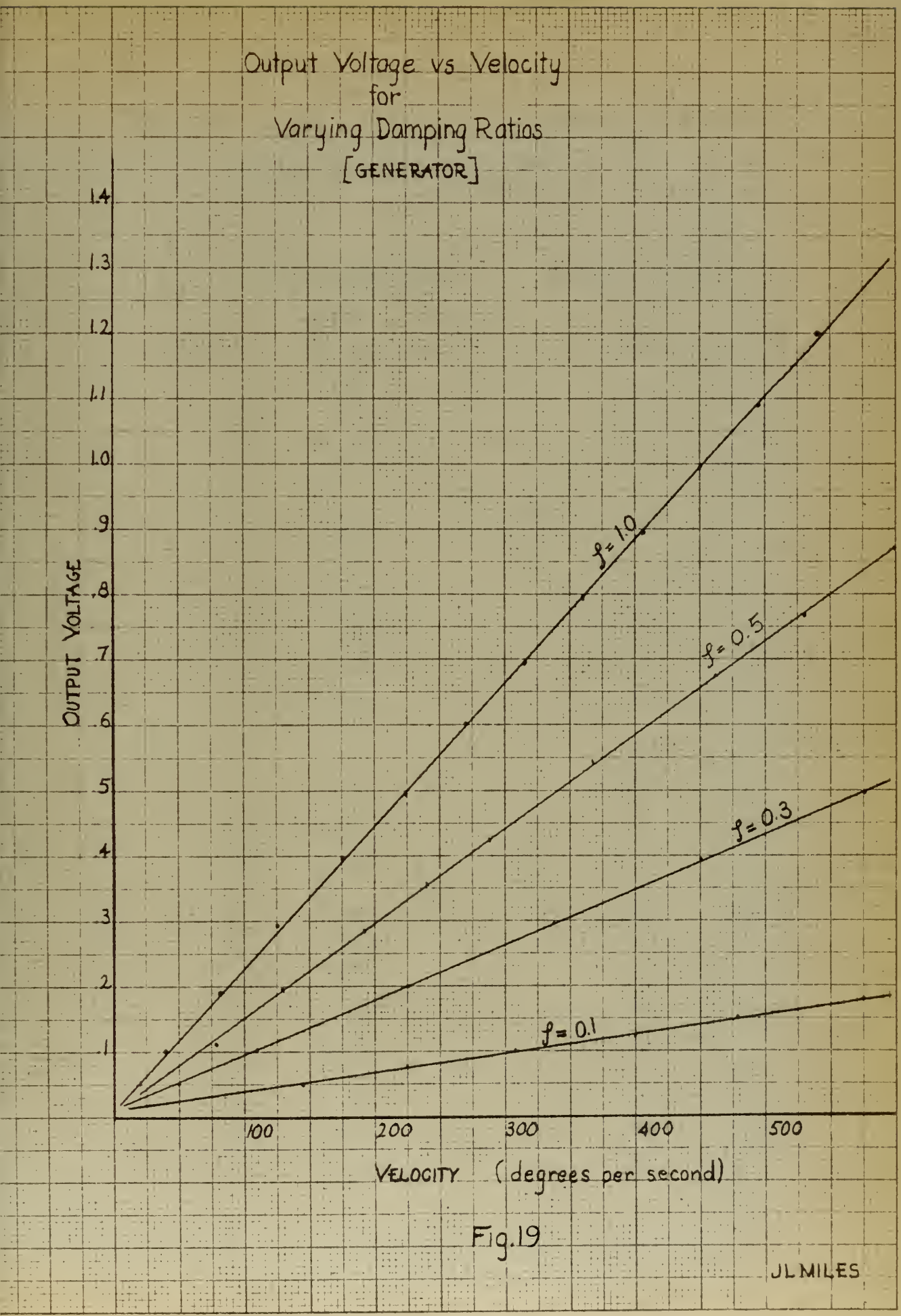
Output Voltage vs Velocity
for
Varying Damping Ratios
[GENERATOR]
OUTPUT VOLTAGE
1.4
1.3
1.2
1.1
1.0
.9
.8
.7
.6
.5
.4
.3
.2
.1
ζ = 1.0
ζ = 0.5
ζ = 0.3
ζ = 0.1
100
200
300
400
500
VELOCITY (degrees per second)
JL MILES

Fig. 19

Table V. Output Voltage of Recording Potentiometer vs. Roll Angle of Turntable.

Output voltage	Roll Angle
0.09	1
0.15	2
0.23	3
0.30	4
0.38	5
0.46	6
0.53	7
0.60	8
0.69	9
0.74	10
0.83	11
0.89	12
0.99	13
1.04	14
1.12	15
1.23	16
1.32	17
1.37	18
1.45	19
1.53	20
1.62	21

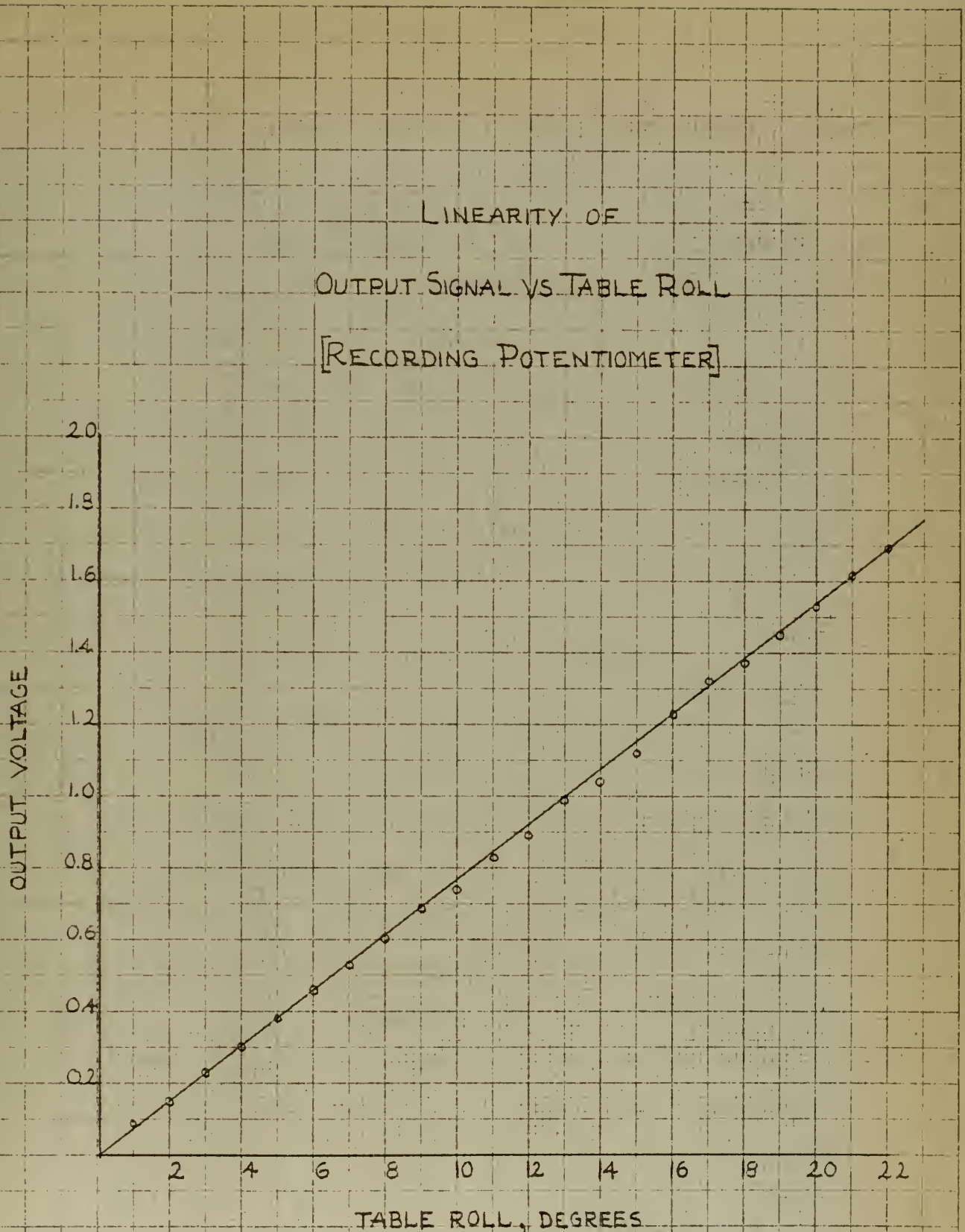

Fig. 20

J.L. MILES

3.3-e Frictional Non-Linearity for Small Angular Velocities.

From the slope of the curve in Figure 20, the value of output voltage per degree of table roll can be determined (0.075 volt per degree).

Values of output voltages can now be converted to degrees of roll of the table, while the angular velocity in degrees per second can be calculated from Brush recordings. The steady-state roll velocity is given by Equation 3.2-3 as

$$\dot{\theta} = b\psi_o/a \quad \text{radians per second}$$

where ψ_o is a fixed displacement of the table.

If the angular velocity is plotted against table displacement, a straight line should result from the above linear relationship. Figure 21 shows the actual curve, which is linear except for small displacements at low frequencies; the velocity being a function of both frequency and the amplitude of displacement. From a study of Figure 21, the presence of frictional dead-space is apparent. This simply means that if experimental data are taken for small angular velocities of the turntable, the frictional effects will be appreciable and will create phase lag in excess to that predicted. This effect can be explained as follows.

The slope of the theoretical curve is

$\frac{\Psi_o}{\dot{\theta}} = a/b \sim a$, the damping factor.

At low velocities, the slope of the vector from the origin to the actual curve is greater, indicating the presence of the added frictional damping. In other words, due to the frictional non-linearity a greater displacement is necessary to obtain the same angular velocity.

Table VI. Angular Velocity vs. Table Displacement.

Angular Velocity		Displacement	
Cycles per second	Degrees per second	Volts	Degrees
0.067	24.1	0.095	1.27
0.159	55.4	0.165	2.20
0.237	85.2	0.230	3.07
0.345	124.2	0.315	4.20
0.526	189.0	0.475	6.31
0.769	277.0	0.685	9.13
0.995	358.0	0.875	11.61
1.100	396.0	0.965	12.86

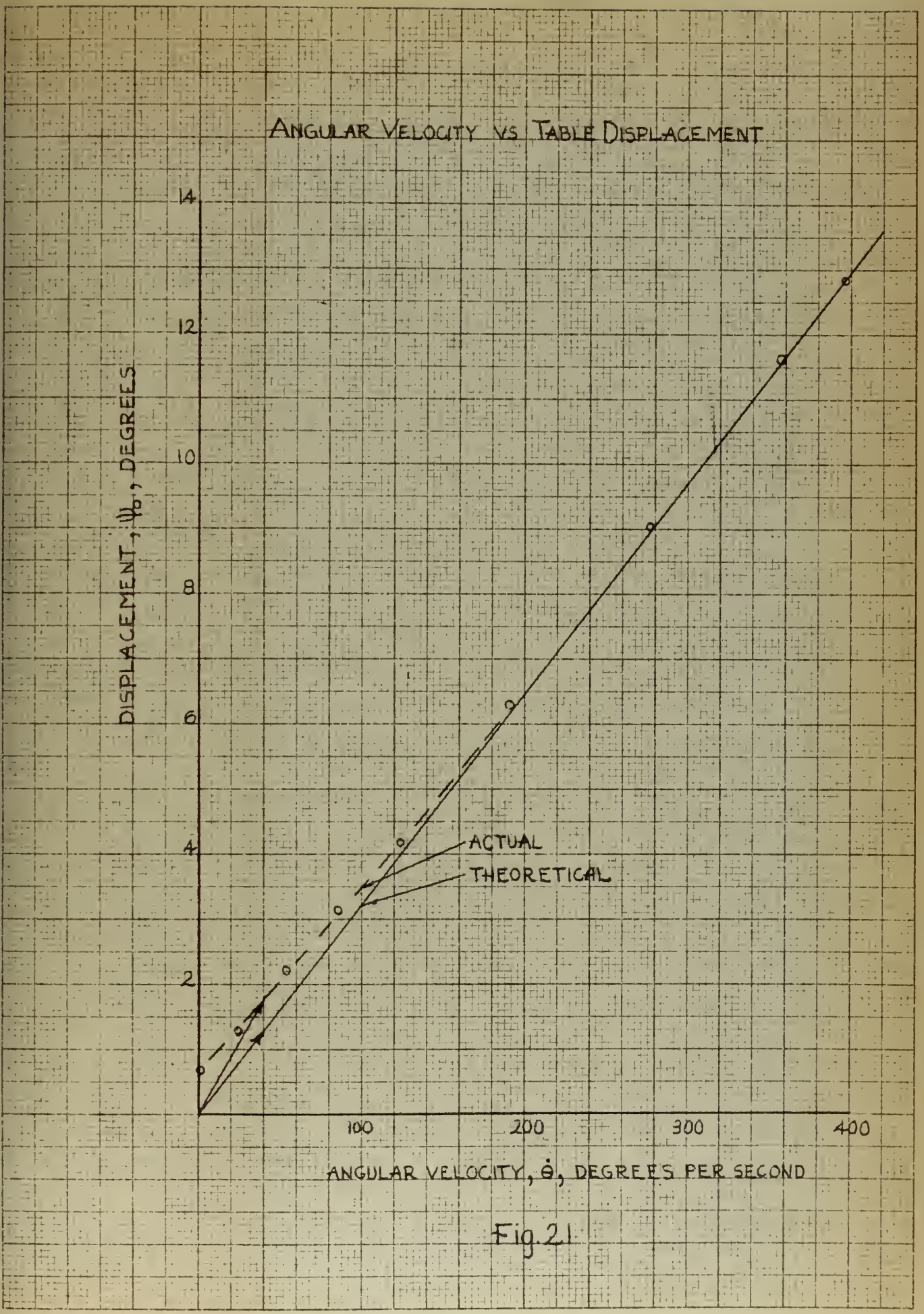
ANGULAR VELOCITY VS TABLE DISPLACEMENT
DISPLACEMENT, ψ_b, DEGREES
14
12
10
8
6
4
2
ACTUAL
THEORETICAL
100
200
300
400
ANGULAR VELOCITY, $\dot{\theta}$, DEGREES PER SECOND

Fig. 21

3.4 The Closed-Loop System and Measuring Apparatus.

The computer, connected as a closed loop, along with the necessary apparatus for measuring the system output to input amplitude ratio and the phase lag, is shown schematically in Figure 22. A photograph of this experimental set-up is shown in Figure 23.

3.4-a The Computer as a Closed-Loop.

The computer amplifier is connected to a 110-volt 60-cycle per second power supply. The amplifier output signal feeds into the control field of the motor, while a constant 60-cycle per second voltage of 110 volts is applied to the main field. The motor shaft, through an 18:1 gear train, drives the turntable. The #1 control transformer, mounted on the turntable shaft, returns a signal to the mixing circuit proportional to the rotation of the turntable. The mixer receives a second signal from the feedback generator which is proportional to the speed of rotation of the table. The mixer output is subtracted from the system input and the resulting signal feeds back into the computer amplifier.

3.4-b The Signal Generating and Phase-Lag Measuring System.

The signal generating and phase-lag measuring

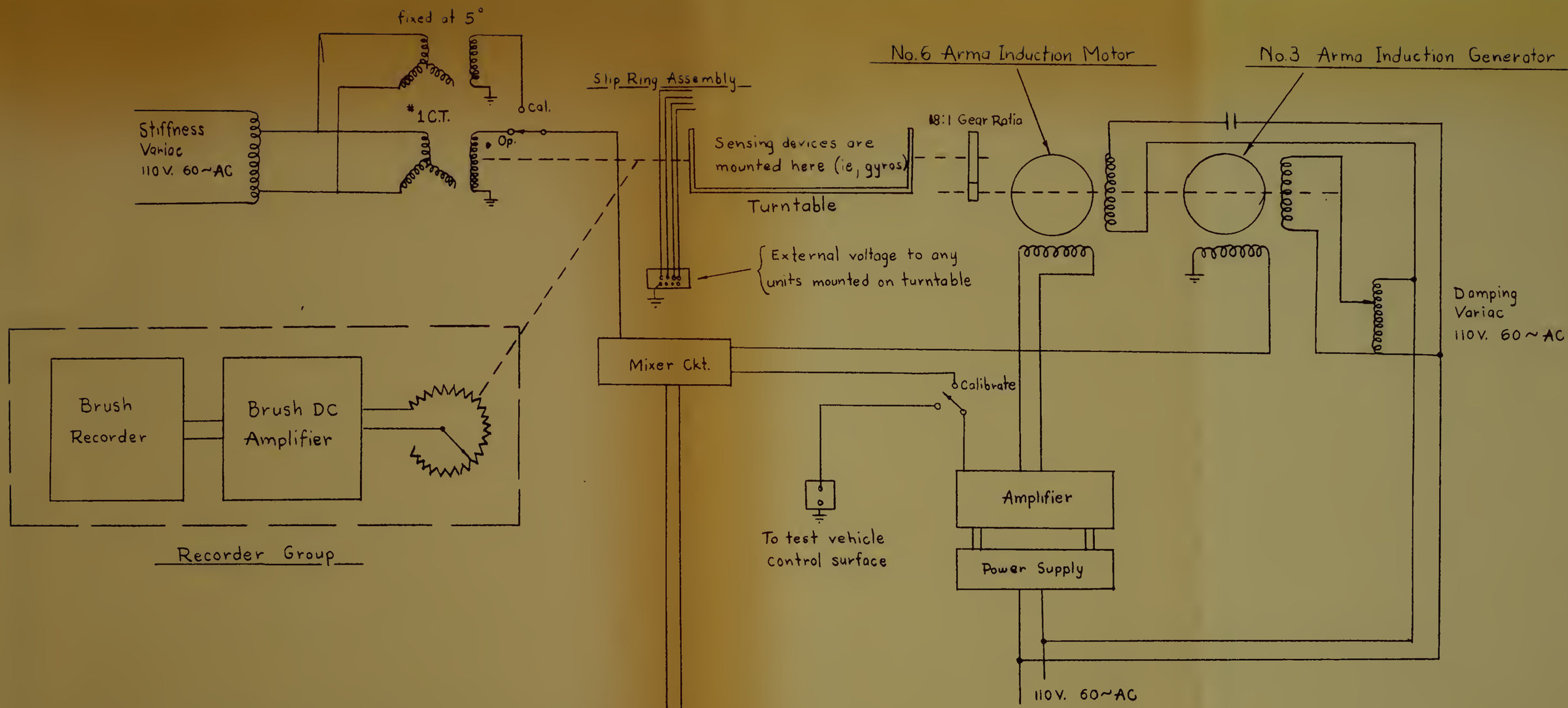

Schematic of Computing System, Including Signal Generating and Recorder Groups

Fig. 22

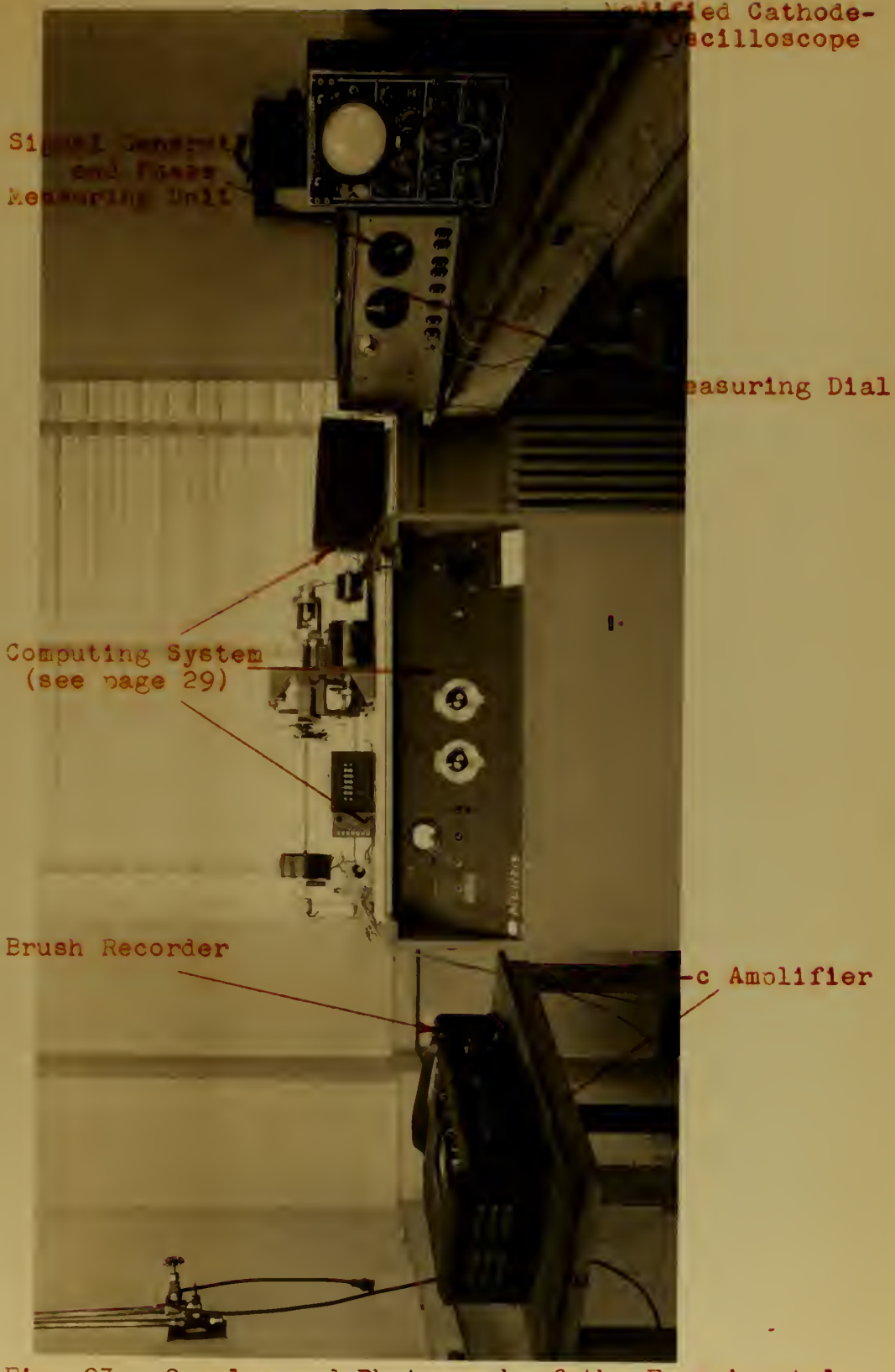

Fig. 23. Overlay and Photograph of the Experimental Set-up.

APPLIED PHYSICS LABORATORY
THE JOHNS HOPKINS UNIVERSITY
8621 GEORGIA AVENUE
PHOTO NUMBER
8981
DATE PRINTED

system consists of a pair of #1 control transformers, two pair of autosyns, two similar d-c amplifiers, two similar demodulators, and a cathode-ray oscilloscope modified for d-c signals. This system, indicated in Figure 22, is shown in detail in Figure 24.

Autosyns 1 and 2 are excited by 26 volts at 8000 cycles per second from an audio signal generator. Control transformer 1 is excited by a 60-cycle per second signal from the amplifier. The rotors of control transformer 1 and autosyn 1 are mechanically coupled and can be driven by a variable-speed motor. The body of control transformer 1 can be rotated by means of a phase-shift knob, and since the case of autosyn 1 is fixed, this causes a phase shift between them. A pointer on the phase-shift knob traverses the face of a circular dial calibrated in degrees.

With the phase-shift knob adjusted to zero on the dial, the voltage across control transformer 2 is adjusted to null by rotation of its input shaft. To obtain the "in-phase" condition of autosyns 1 and 2, the voltmeter was connected across the autosyn pair and again adjusted to a voltage null. This was repeated for autosyns 3 and 4 after setting the table to zero degrees of rotation.

The modulated signal of feedback autosyn 4 is fed to the d-c amplifier and demodulator (2). The

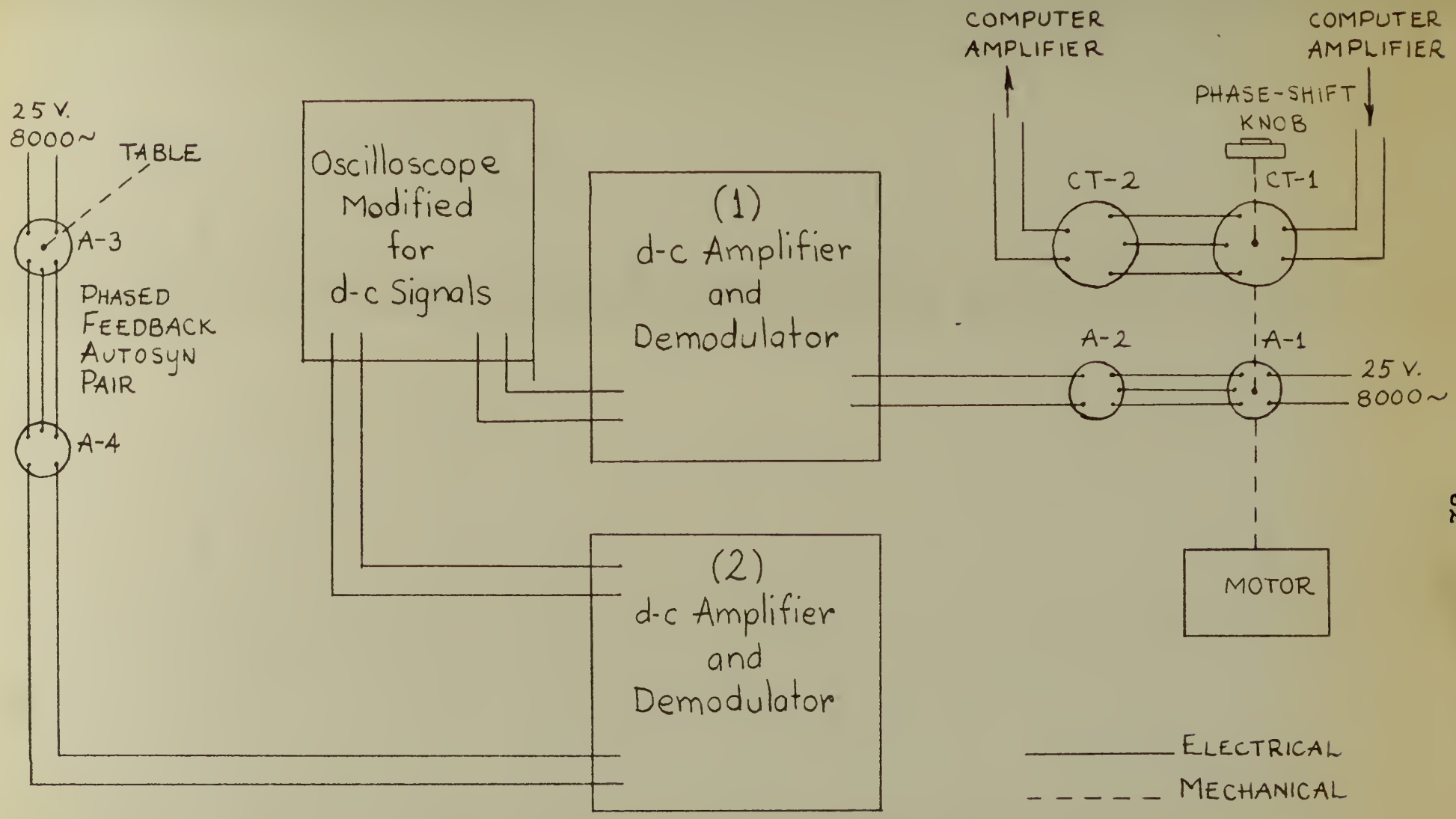

THE PHASE-LAG MEASURING SYSTEM

Fig. 24

output signals of the two d-c amplifiers and demodulators are applied to the cathode-ray oscilloscope modified for d-c signals. Since these two signals are sinusoidal, a Lissajou figure appears on the cathode-ray tube which is a single loop. When the two sinusoidally modulated signals are in phase, the Lissajou figure closes to a single straight line.

When the phase-shift knob is set to zero on the dial, the modulated signals from control transformer 2 and autosyn 2 are in phase for all driving speeds. A phase lag occurs through the computer loop, and the output-modulated signal from autosyn 4 will lag the input signals. If the phase-shift knob of control transformer 1 is rotated in such a manner as to cause the input signal of control transformer 2 to lead the input signal of autosyn 2 by an amount equal to the phase lag that occurs in the computer, modulated signals from autosyns 2 and 4 are in phase.

This in-phase condition is readily apparent when the loop of the Lissajou figure on the cathode-ray tube becomes a straight line. Thus, to determine the phase lag, it is only necessary to turn the phase-shift knob until the lissajou figure becomes a straight line. The measured phase lag is then read directly from the circular dial.

3.4-c The Amplitude Measuring System.

The amplitude measuring system consists of a recording potentiometer, driven by the turntable shaft, a d-c supply, a zero-positioning potentiometer, a d-c Brush amplifier and a Brush recorder. This system is shown in Figure 25.

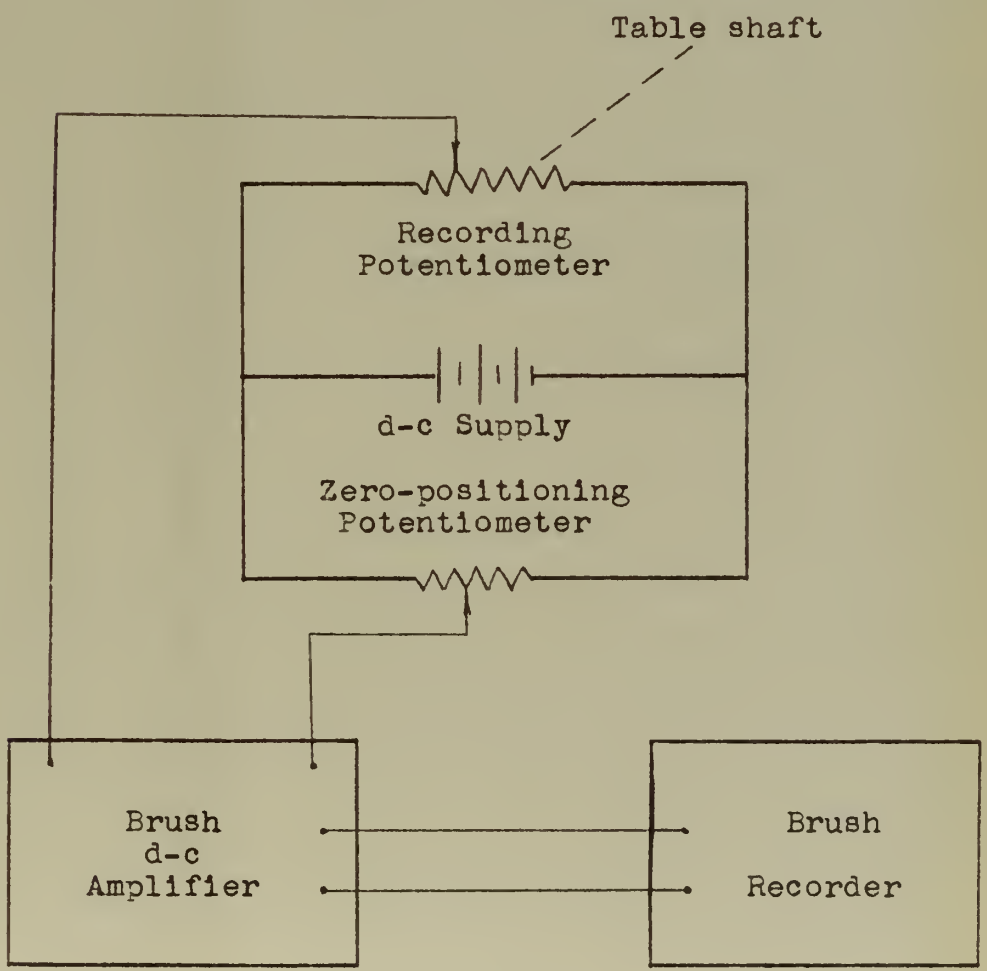

Fig. 25. The Amplitude Measuring System.

The d-c supply was connected to the recording potentiometer in parallel with the zero-positioning potentiometer. The zero-positioning potentiometer was then adjusted so that the potential, and thus the output of the recording potentiometer, was zero when the table was at rest at zero degrees of rotation. The d-c Brush amplifier was used to amplify the output signal from the recording potentiometer. Finally, a graph of the amplitude as a function of time was recorded on paper tape in the Brush recorder.

The Brush recording not only supplies a plot of the output amplitude, but also provides a means of measuring the actual input signal frequency. From the recorder tape, the number of cycles and the elapsed time are both obtained to determine the frequency in cycles per second.

At very low frequencies the amplitude ratio of output to input is essentially unity. Therefore, the amplitude of the input signal was adjusted while the table was driven at the slowest possible speed. This was done by adjusting the gain of the Brush amplifier until the Brush recorder pen oscillated over a peak-to-peak distance of the desired amount.

3.5 The Experimental Results.

The experimentally determined amplitude-ratio and phase-lag data are recorded in Tables VII to X.

These tests were conducted with the computer calibrated for the same values of a and b, and thus the same damping ratios, as were used in the theoretical calculations of Section 2.7. This facilitates correlation of theoretical and experimental results. The phase-lag data are plotted versus frequency in Figures 26 and 27, and the amplitude ratio data are plotted versus frequency in Figure 28.

The re-plotting of Figure 26 was necessary because of the phenomena discussed in Section 3.3-e. The discrepancies between the experimental and theoretical phase lags at low frequencies was not believed to be accurate. Upon investigation it was discovered that if the initial displacement of the table was increased, the additional phase lag, due to frictional effects, was eliminated. The corrected data was then plotted in Figure 27 showing the close correlation expected at lower frequencies.

Figures 27 and 28 indicate the effect of varying the damping ratio, ζ, at a constant resonant frequency. To obtain a more complete picture of the system performance, a sequence of tests was conducted at various resonant frequencies with a fixed damping ratio of 0.17. These data, recorded in Tables IX and X, are plotted in Figures 29 and 30.

Table VII. Experimental Phase-Lag Data for Varying Damping Ratios at Constant Resonant Frequency.

f = 0.17

Frequency in cycles/second	Phase Lag in degrees
0.25	8
0.57	12
0.90	17
1.25	24
1.70	44
1.80	55
1.92	77
2.00	93
2.10	103
2.16	119
2.35	141
2.61	156
3.22	169
3.90	175
5.00	180
0.50*	5
1.00*	13
1.20*	18

f = 0.30

Frequency in cycles/second	Phase Lag in degrees
0.34	8
0.55	13
0.84	20
1.38	38
1.60	51
1.86	76
2.00	92
2.15	114
2.50	137
3.00	152
3.46	162
3.93	168
5.00	176
0.30*	5
0.50*	9
0.70*	14
1.00*	21

f = 0.50

Frequency in cycles/second	Phase Lag in degrees
0.25	8
0.50	16
0.80	26
1.05	36
1.35	51
1.65	68
1.85	84
2.20	102
2.45	115
2.86	132
3.30	144
4.00	155
4.71	162
5.62	169
6.69	176

f = 1.00

Frequency in cycles/second	Phase Lag in degrees
0.23	13
0.44	25
0.67	36
0.91	49
1.20	62
1.48	73
1.75	82
2.00	93
2.50	106
3.00	118
3.60	128
4.24	138
4.80	146
5.94	155
7.65	166
8.75	172

* Corrected data.

Table VIII. Experimental Amplitude-Ratio Data for Varying Damping Ratios at Constant Resonant Frequency.

f = 0.17

Frequency in cycles/second	Amplitude ratio
0.25	1.010
0.57	1.080
0.90	1.250
1.25	1.600
1.70	2.500
1.80	2.900
1.92	3.300
2.00	3.500
2.10	3.040
2.16	2.600
2.35	1.900
2.61	1.250
3.22	0.560
3.90	0.335
5.00	o.170
7.02	0.086

f = 0.30

Frequency in cycles/second	Amplitude ratio
0.34	1.020
0.55	1.080
0.82	1.160
1.38	1.520
1.60	1.750
1.86	1.900
2.00	1.850
2.15	1.650
2.50	1.200
3.00	0.700
3.46	0.455
3.93	0.305
5.00	0.165
7.08	0.082

f = 0.50

Frequency in cycles/second	Amplitude ratio
0.23	0.985
0.44	0.970
0.67	0.910
0.91	0.860
1.20	0.780
1.48	0.705
1.75	0.620
2.00	0.540
2.50	0.420
3.00	0.320
3.60	0.240
4.24	0.180
4.80	0.145
5.94	0.095
6.67	0.080
7.65	0.056
8.75	0.043

f = 1.00

Frequency in cycles/second	Amplitude ratio
0.25	1.000
0.50	1.035
0.80	1.080
1.05	1.120
1.35	1.180
1.65	1.230
1.85	1.205
2.20	1.000
2.45	0.820
2.86	0.610
3.30	0.450
4.00	0.270
4.71	0.185
5.62	0.130
6.69	0.087
8.23	0.054

Table IX. Experimental Phase-Lag (Ø) Data for a Constant Damping Ratio at Various Resonant Frequencies.

Cps	Degrees	Cps	Degrees	Cps	Degrees
0.20	10	0.50	5	0.14	1
0.30	19	1.00	13	0.78	4
0.39	36	1.20	18	1.50	7
0.48	84	1.70	44	2.34	13
0.55	107	1.80	55	2.80	17
0.60	127	1.92	77	3.33	24
0.70	145	2.00	93	3.57	30
0.80	154	2.10	103	3.89	41
0.90	159	2.16	119	4.28	57
1.20	168	2.35	141	4.50	74
		2.61	156	4.67	92
		3.90	175	4.85	116
		5.00	180	5.25	136
				5.46	150
				5.95	160
				6.65	171

Table X. Experimental Amplitude-Ratio (A) Data for a Constant Damping Ratio at Various Resonant Frequencies.

Cps	A	Cps	A	Cps	A
0.20	1.20	0.25	1.010	0.14	1.001
0.30	1.55	0.57	1.080	0.78	1.010
0.39	2.10	0.90	1.250	1.50	1.050
0.48	2.80	1.25	1.600	2.34	1.300
0.55	2.30	1.70	2.500	2.80	1.480
0.60	1.60	1.80	2.900	3.33	1.800
0.70	0.90	1.92	3.300	3.57	2.150
0.80	0.55	2.00	3.500	3.89	2.660
0.90	0.40	2.10	3.040	4.28	3.500
1.20	0.18	2.16	2.600	4.50	4.200
		2.35	1.900	4.67	4.330
		2.61	1.250	4.85	3.700
		3.22	0.560	5.25	3.000
		3.90	0.335	5.46	2.205
		5.00	0.170	5.95	1.500
		7.02	0.086	6.65	0.805
				7.90	0.400

Damping ratio of 0.17.
Resonant frequencies of 0.5, 2.0, and 4.5 respectively.

J.L. Miles
1st Lt USMC

12
24
36
48
60
72
84
96
108
120
132
144
156
168
180

PHASE ANGLE, ψ (degrees)

ζ=.17
ζ=.3
ζ=.5
ζ=1.0

Phase Lag vs Frequency
for
Closed Loop Second Order System

$-\phi = \arctan\left[\frac{\omega}{K-\omega^2 T}\right]$

o- - -o- - -o } Experimental
+ - - + - - + }

——— Theoretical

ζ=1.0
ζ=0.5
ζ=0.3
ζ=0.17

Fig. 26

1 2 3 4 5 6 7 8 9 1 2 3 4 5 6 7 8 9 10
2 3 5 7 10 2 3 5 7 9

FREQUENCY (cycles per second)

389-62L KEUFFEL & ESSER CO.
Semi-Logarithmic, 2 Cycles X 5 to the inch.
MADE IN U. S. A.

J.L. Miles
1st.Lt. USMC

$\zeta = .17$

$\zeta = .3$

$\zeta = .5$

$\zeta = 1.0$

PHASE ANGLE, Φ (degrees)

12
24
36
48
60
72
84
96
108
120
132
144
156
168
180

Phase Lag vs Frequency
for
Closed Loop Second Order System

$-\Phi = \arctan\left[\frac{\omega}{k-\omega^2 T}\right]$

o – – o – – o + – – + – – + } Experimental

Theoretical

Fig. 27

1 2 3 5 7 10 2 3 5 7 9

FREQUENCY (cycles per second)

$\zeta = .17$

$\zeta = .3$

$\zeta = .5$

$\zeta = 1.0$

A - AMPLITUDE RATIO

Amplitude Ratio vs Frequency
for
Closed Loop Second Order System

$$A = \frac{1}{\sqrt{\left[1 - \frac{m\omega^2}{k}\right]^2 + \left[\frac{\omega}{k}\right]^2}}$$

Experimental
Theoretical

Fig 28

J.L. Miles
1st Lt USMC

FREQUENCY, CPS

KEUFFEL & ESSER CO.
Semi-Logarithmic, 2 Cycles X 6 to the ½ Inch.
MADE IN U.S.A.

J.L. Miles
1st.Lt. USMC

PHASE ANGLE, ψ (degrees)

12
24
36
48
60
72
84
96
108
120
132
144
156
168
180

2 3 .5 7 1.0 2 3 5 7 9

FREQUENCY (cycles per second)

Phase Lag vs Frequency
for
Closed Loop Second Order System
at
Various Resonant Frequencies

$-\phi = \arctan\left[\frac{\omega}{K-\omega^2 T}\right]$

o--o--o Experimental
——— Theoretical

$f = .17$

Fig. 29

Amplitude Ratio vs Frequency
for
Second Order System
of
Various Resonant Frequencies

$$A = \frac{1}{\sqrt{\left[1 - \frac{T\omega^2}{K}\right]^2 + \left[\frac{\omega}{K}\right]^2}}$$

$f = .7$

Theoretical

Experimental

Fig. 30

4. CORRELATION OF THE EXPERIMENTAL AND THEORETICAL RESULTS.

4.1 Experimental versus Second-Order Theory.

The experimental phase-lag curves for the closed-loop system are plotted in Figures 26 and 28, from the data of Tables VII and IX. The phase lag in degrees is plotted as a function of the input signal frequency in cycles per second. Two sets of curves were obtained; one at constant resonant frequency, with damping ratios varying from 0.17 through 1.0, and the other at a constant damping ratio, with the resonant frequency varying from 0.5 to 4.5 cycles per second. Theoretical second-order system phase-lag curves, with these same values of ζ and ω, are also plotted on Figures 26 and 28.

At low frequencies, there is a high degree of correlation between the experimental and the theoretical results. However, as the frequency increases beyond resonance, the experimental phase shift lags, more and more, that predicted by the second-order system theory. This deviation clearly indicates the presence of an additional linear delay in the system, since the increasing phase lag appears as a function of frequency.

The experimental and theoretical second-order system amplitude-ratio curves are plotted in Figures 28

and 30, from the data of Tables VIII and X. The experimental results indicate greater over-shoot than expected, since the maximum values of the amplitude ratio are greater than predicted. Beyond the resonant frequency, the negative slopes of the experimental curves are greater than the predicted slopes. Also, from Figure 30, as the resonant frequency increases, the peak values of the amplitude ratio increase. All of these results lend credence to the existence of an additional linear delay, said delay being a function of frequency.

It is difficult to quantify the effectiveness of the system, since the results are dependent on the calibration. The damping ratio, ζ, is a function of the calibration constants, a and b. Thus, as the stiffness and damping of the system are altered, the results vary. However, the following conclusions seem justified from the results obtained: 'No appreciable error appears in the phase lag below 2 cycles per second. For the frequency range from 2 to 5 cycles per second, the error increases from zero to 6 or 7 per cent. Beyond this frequency, the error increases more rapidly.

4.2 Experimental versus Third-Order Theory.

Assuming that the additional time delay of the system is in the form of a distinct, independent time constant, its magnitude can be determined readily

by trial and error approximations. This can be done by substituting values for T_2 into the third-order expressions developed in Section 2.8, until these calculated results fit the experimental curves. T_1 and K retain their original values, since they are functions of the calibration constants, a and b.

The value of T_2 was first estimated at 3 milliseconds and found to be too small. After two more trials, the value of 5 milliseconds resulted in a calculated point that plotted directly on the corresponding experimental curve. Further calculations led to a remarkable correlation between the third-order and experimental curves. This was true for both the phase-shift and amplitude-ratio curves.

The calculated data are tabulated in Tables XI and XII and plotted with the experimental results in Figures 31 and 32.

Table XI. Calculated Phase-Lag Data for a Third Order System.

Frequency in Cycles/second	Phase Lag, ϕ, in Degrees			
	ζ=0.17	ζ=0.30	ζ=0.50	ζ=1.00
0.2	2.0	3.5	5.8	11.4
0.5	5.1	9.2	14.9	28.2
1.0	12.3	21.5	33.9	53.8
1.5	28.2	45.6	61.1	75.0
2.5	152.0	135.0	120.6	108.0
3.0	167.0	152.8	137.7	119.0
4.0	176.7	168.0	155.3	135.2
5.0	-----	175.0	165.1	146.6
7.0	-----	-----	176.6	162.0

Table XII. Calculated Amplitude-Ratio Data for a Third-Order System.

Frequency in Cycles/Second	Amplitude Ratio, A			
	ζ=0.17	ζ=0.30	ζ=0.50	ζ=1.00
0.5	1.065	1.060	1.035	0.950
1.0	1.310	1.250	1.130	0.820
1.5	2.060	1.670	1.210	0.680
2.0	3.590	1.860	1.120	0.520
2.5	1.490	1.130	0.770	0.410
3.0	0.750	0.670	0.535	0.320
4.0	0.325	0.310	0.285	0.205
5.0	0.185	0.180	0.170	0.140
7.0	0.088	0.085	0.082	0.070
10.0	0.040	0.038	0.037	0.035

KEUFFEL & ESSER CO.
Semi-Logarithmic, 2 Cycles × 5 to the Inch.
MADE IN U. S. A.

JJL Miles

f = .17
f = .3
f = .5
f = 1.0

Phase Angle in Degrees

12
24
36
48
60
72
84
96
108
120
132
144
156
168
180

Phase Lag vs. Frequency
for
Third Order System

$$-\phi = \arctan \frac{\omega - \omega^3 T_1 T_2}{K - \omega^2 (T_1 + T_2)}$$

where $T_2 = 0.005$ sec.

——— Theoretical

o o o o o
+ + + + + } Experimental

2 3 5 7 10 2 3 5 7 10

Frequency, cps

Fig. 31

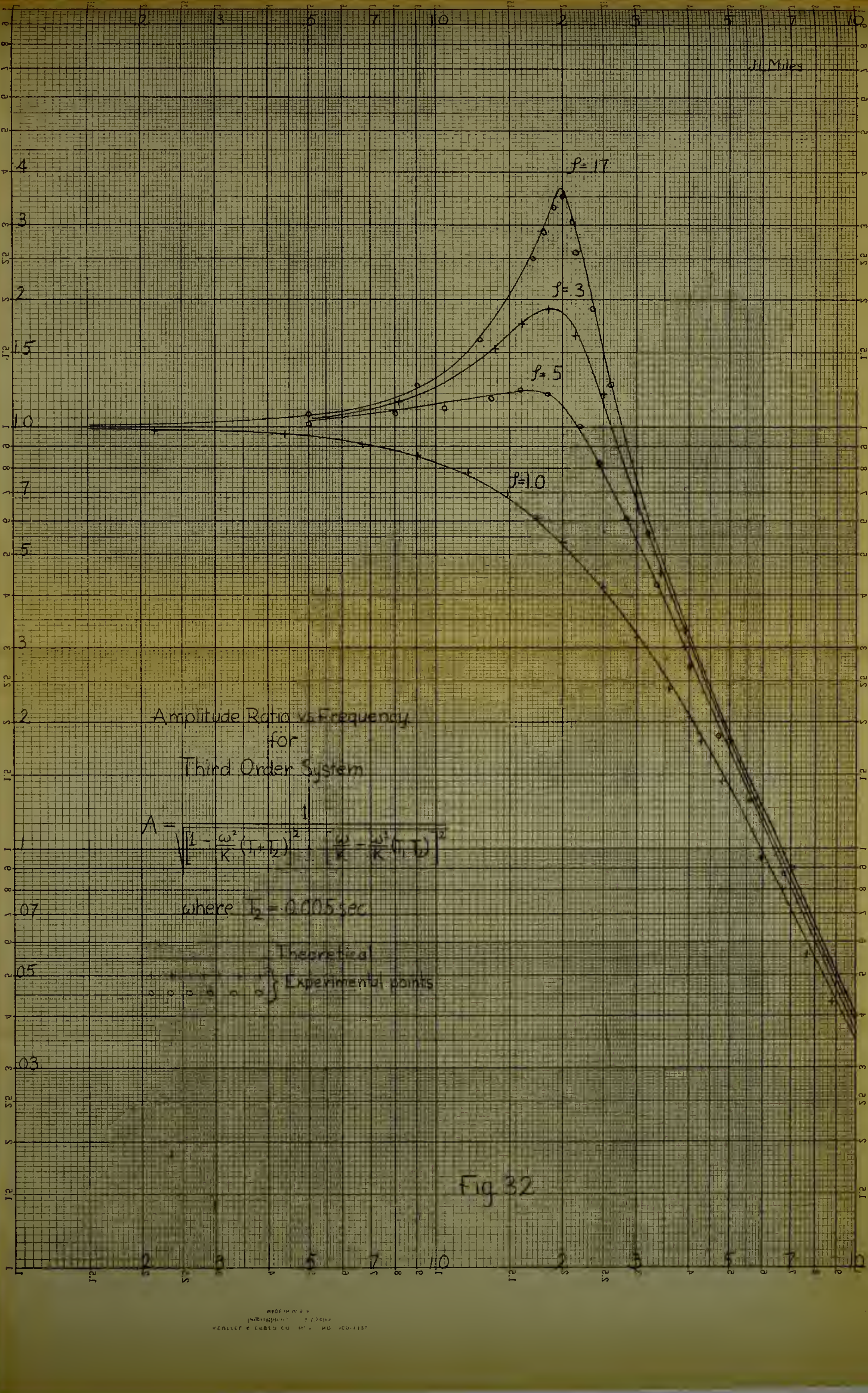
Ji Miles
f= 17
f= 3
f= 5
f=1.0
Amplitude Ratio vs Frequency
for
Third Order System
$A = \frac{1}{\sqrt{\left[1 - \frac{\omega^2}{K}(T_1+T_2)\right]^2 + \left[\frac{\omega}{K} - \frac{\omega^3}{K}(T_1 T_2)\right]^2}}$
where $T_2 = 0.005$ sec
Theoretical
Experimental points

Fig 32

5. ISOLATION OF THE ADDITIONAL DELAY.

5.1 Discussion of Delay.

Having established the presence of an additional time lag, an attempt to isolate and measure the delay is believed to be incumbent upon an investigation such as this. The assumption has been made, and partially substantiated, that the delay is distinct and independent. This indicates the already logical source of the additional delay--the induction motor.

In Section 2.4, two forms were given for the transfer function of an a-c, two-phase, induction motor. The second of these, Equation 2.4-2, contained two distinct delays, one mechanical and one electrical. The first, Equation 2.4-1, has been used in this analysis, until now, for two reasons: (1) The conventional texts, for the most part, have treated the electrical constant as negligible or have ignored it. (2) Utilization of the system to date has been based upon the system transfer function developed in Section 2.3, which is devoid of any electrical delay. However, now that a third-order system is apparent, the presence of an electrical delay in the motor seems very likely.

In Reference 5, Mr. Brown substantiates this assumption and states the magnitude of the delay as equivalent to the ratio of rotor inductance to rotor resistance. A similar transfer function for a d-c

motor (Reference 1, page 128) gives the second or electrical delay as the ratio of the field inductance to resistance. Dr. Sobczyk, in his analysis in Reference 10, concludes that the a-c motor is effectively equivalent to a demodulating device followed by a d-c motor. Thus, if an analogy is drawn to the d-c treatment of Brown and Campbell (Reference 1, page 128), the following equivalent circuit results from the motor as connected to the amplifier.

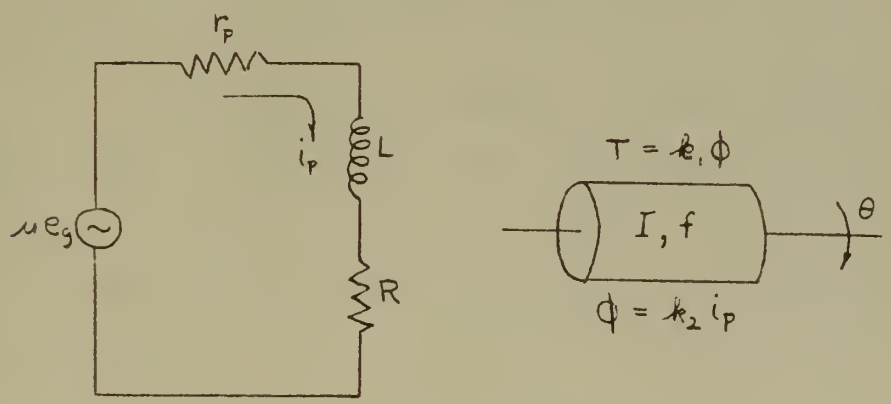

Fig. 33. Equivalent Circuit of the Motor and the Amplifier Output Stage.

The transfer function of such a system is of the form,

$$\frac{\theta}{E}(s) = \frac{K}{s(T_m s+1)(T_e s+1)} \qquad (5.1\text{-}1)$$

where T_m is the mechanical delay due to the inertia and viscous friction, while T_e is an electrical delay. Considering only the electrical circuit,

$$\mu e_g = r_p i_p + R i_p + L \, di_p/dt \qquad (5.1\text{-}2)$$

which is transformable to

$$\mu E(s) = I(s)\left[r_p + R + Ls\right] \qquad (5.1\text{-}3)$$

Thus,

$$\frac{I}{E}(s) = \frac{\mu}{(r_p + R) + Ls} \qquad (5.1\text{-}4)$$

Since the rotor torque is proportional to the current,

$$\frac{T}{E}(s) = \frac{K}{(L/r_p + R)s + 1} = \frac{K}{T_e s + 1} \qquad (5.1\text{-}5)$$

Obviously, the process of calculating this delay would be difficult and laborious; and since the magnitude of the delay is believed to be approximately 5 milliseconds, a method of measuring it experimentally was devised.

5.2 Experimental Procedure.

To effect the measurement of the electrical delay it was necessary to attach a transducer element to the output shaft of the motor. This enabled recording of the torque-to-input transfer function of Equation 5.1-5.

The transducer used was a Model G1-48-675 of the Statham Laboratories (Reference 11).

The Statham Transducer Element. When physical measurements are made it is often necessary to transduce

mechanical parameters to sensible electrical units. In force or torque studies, a displacement must actuate a transducing element which will yield an electrical signal proportional to the torque. The electrical signal can then be transmitted to an electrical recording system. To satisfy these needs, Statham Laboratories has developed a basic displacement transducer in which displacements up to 0.0015 inches are caused to produce sensible resistance changes proportional to the displacement.

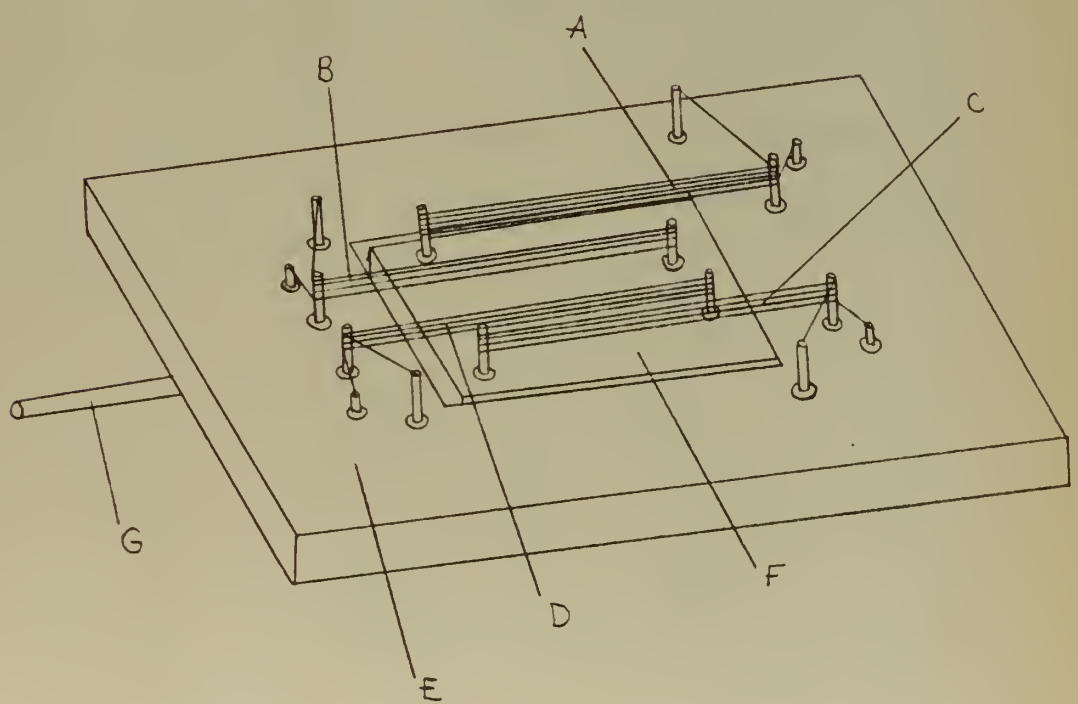

Fig. 34. The Statham Transducer.

The displacement transducer element is shown in Figure 34. It consists of a frame, E, supporting a movable armature, F, by two thin cantilever plates. Four sets of constantan filaments, A, B, C, D, are strung under initial tension between the frame and armature in the manner shown. When the armature is displaced longitudinally, two of the sets of filaments will be elongated, while the other two sets will shorten. The elongated filaments will increase in resistance, while the resistance of the shortened filaments will decrease. The change in resistance of the filaments will be proportional to their change in length. The transducer is so wired that the filaments are connected in a Wheatstone bridge circuit, as shown in Figure 35. The resistance change of the filaments alters the electrical balance of the bridge so that an electric current is caused to flow in the output circuit.

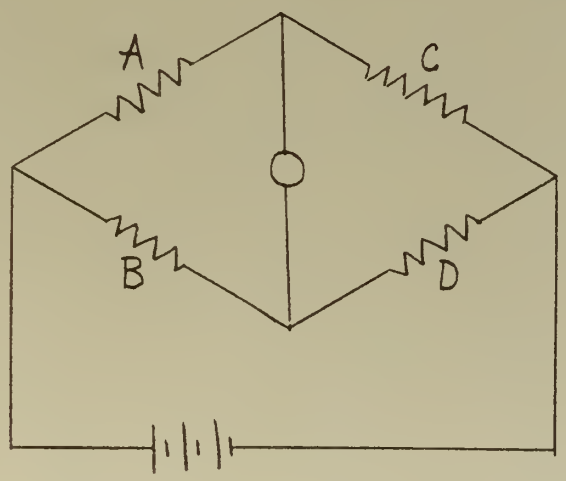

Fig. 35. The Bridge Circuit of the Transducer.

The cantilever plates which support the armature are mounted on the under side of the element. G is the linkage pin by which movement is transmitted to the armature. A fixed stud on the armature rides within a square hole in the undercarriage, so accurately sized that the armature can move a maximum of 0.0015 inches in either direction. A "trimmer" resistor is placed in series with one of the bridge elements. It is adjusted after assembly of the transducer to equalize the resistance of the four elements of the bridge. If the bridge is balanced at zero output before the displacement is applied, the unbalance electrical output of the bridge will bear an accurate, linear relationship to the displacement.

Procedure. The transducer was attached to the motor shaft as shown by the photograph of Figure 36. The rotor torque is transmitted through the linkage pin and produces a displacement of the armature which is directly proportional to the torque. In the model used, a torque of 48 ounce-inches is required to displace the armature 0.0015 inches.

It should be emphasized here that the maximum displacement of the rotor shaft is 0.0015 inches. Thus, the motor is essentially stationary and independent of the forces of inertia and viscous friction. In other words, if the torque equation is considered;

$$T = I\ddot{\theta} + f\dot{\theta} + k\theta \qquad (5.2\text{-}1)$$

it is apparent that the torque from the inertial and frictional terms provides a negligible contribution when compared to the third term.

The amplitude and phase measuring systems are essentially the same as described in Section 3.4. The output of the transducer element is fed through a d-c amplifier and demodulator to the cathode-ray oscilloscope, where its phase is compared with the phase of the input signal. The Brush recorder was replaced by the Miller recording system, since the frequencies were higher. At the higher frequencies, the Brush recorder contributes to the phase lag, while the Miller recorder has the following desired characteristics: The amplitude response is flat and the phase lag negligible over the frequency range used.

The calculated and experimental data are tabulated in Table XIII and plotted in Figure 37.

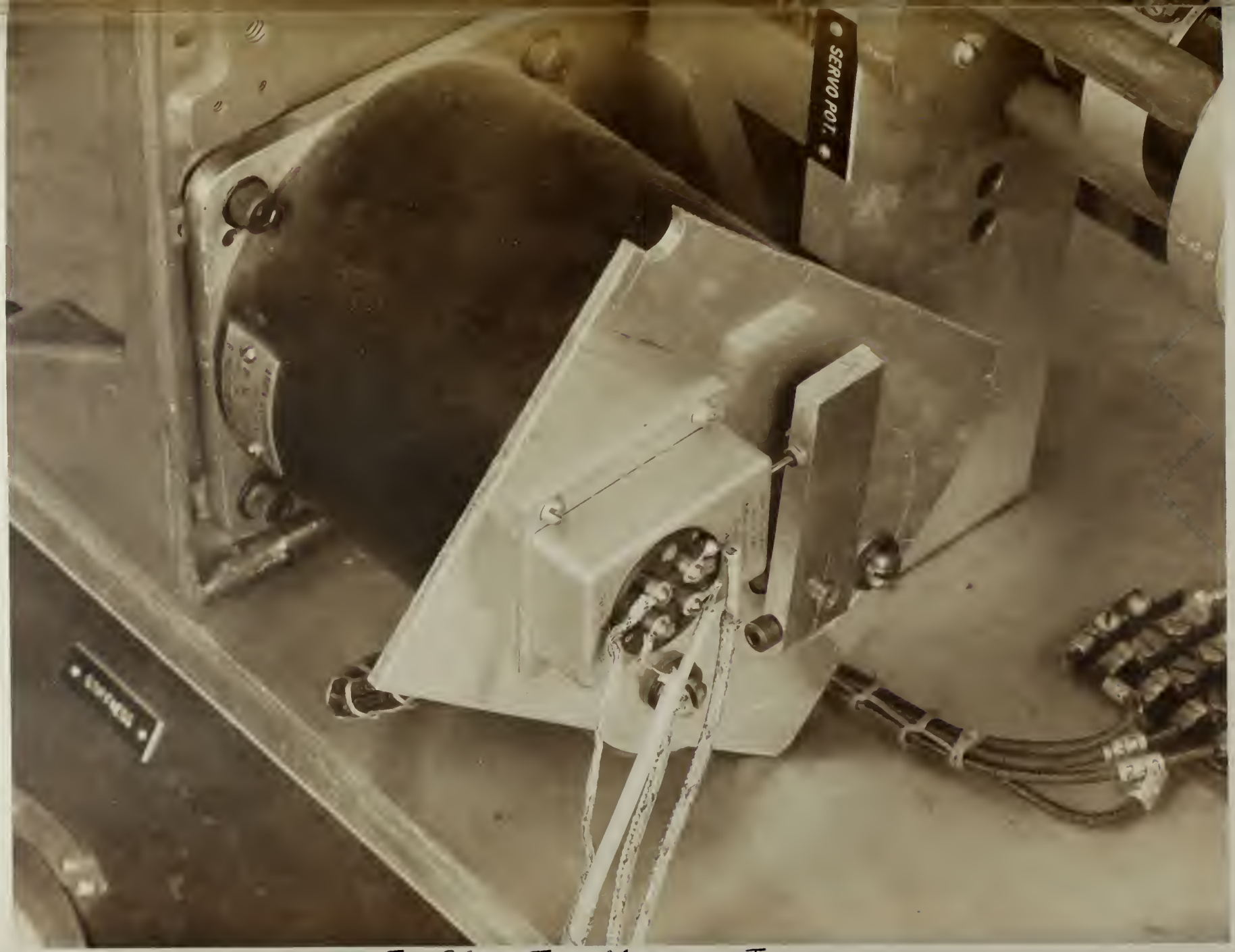

FIG. 36. THE MOUNTED TRANSDUCER

APPLIED PHYSICS LABORATORY
THE JOHNS HOPKINS UNIVERSITY
THIS PHOTOGRAPH ON FILE AT
8621 GEORGIA AVENUE
PHOTO NUMBER
9905
DATE PRINTED

Table XIII. Calculated and Experimental Data for a First-Order System.

$$A = \frac{1}{\sqrt{1 + (\omega T)^2}} \qquad \phi = -\arctan \omega T \qquad T = 0.005$$

CALCULATED

f	ω	A	∅
1	6.28	1.000	1.8
3	18.84	.996	5.4
5	31.40	.990	8.9
10	62.80	.955	17.4
15	94.20	.905	25.2
20	125.60	.847	32.1
25	157.00	.787	38.1
30	188.40	.730	43.3
40	251.20	.623	51.4

EXPERIMENTAL

f	A	∅
2.0	.998	4.0
4.5	.995	7.5
8.5	.960	14.5
11.0	.940	18.0
14.0	.910	23.0
19.0	.850	30.0
23.0	.800	35.0
28.0	.750	40.0
30.0	.720	43.0

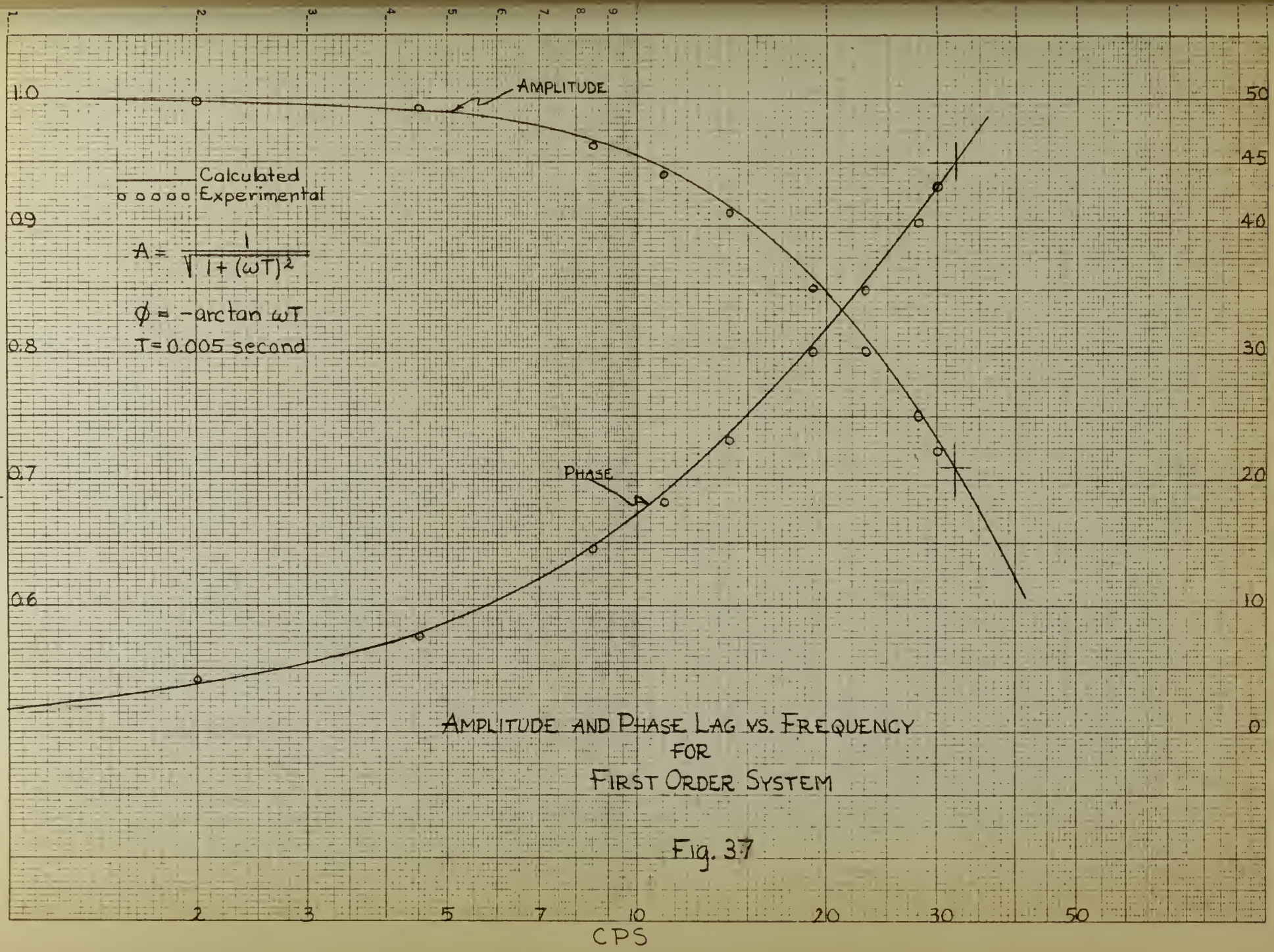

AMPLITUDE AND PHASE LAG VS. FREQUENCY
FOR
FIRST ORDER SYSTEM

Fig. 37

5.3 Correlation of Results.

From Figure 37, the correlation of the calculated and experimental results appears to be very good. The physical limitations of the experimental apparatus allowed measurements to only 30 cycles per second. However, this is sufficient to verify the magnitude of the delay. For a first-order system, a phase lag of 45 degrees occurs at the frequency, $\omega = 1/T$. The amplitude attenuates 3 decibels, or to approximately 0.7 of its original magnitude, at this same frequency. When $T = 0.005$, $\omega = 200$ and, therefore, the 45 degree phase shift occurs at approximately 32 cycles per second.

6. CONCLUSIONS AND RECOMMENDATIONS

As a result of this investigation, the author has reached the following conclusions:

(1) The correlation between the experimental results and those calculated for a second-order system is very good for frequencies to 2 cycles per second. Above this frequency, the experimental phase lag is greater than predicted, but remains less than 10 per cent in error out to 5 cycles per second. Above 5 cycles per second, the discrepancy increases rapidly.

(2) The order of the computing system is greater than the second, as indicated by the phase lag and output signal attenuation being greater than predicted for a second-order system.

(3) The presence of an additional linear delay indicates the computer is a third-order system.

(4) The additional delay is an "electrical" delay within the induction motor and has a magnitude of 5 milliseconds.

The following recommendations are respectfully submitted:

(1) Additional phasing capacitors should be added to the Arma motor circuits to insure that the

torque is independent of speed over the useful speed range of the motor (Reference 9).

(2) A study should be made with the objective of eliminating or compensating for the additional delay. Perhaps one approach is to increase the impedance of the amplifier stage and thus, decrease the ratio of inductance to resistance.

(3) In order to quantify the effectiveness of the computer as a second-order system, additional sequences of frequency responses are necessary over varying ranges of frequency and damping ratios. Perhaps a worthy extension of this investigation might be the interpretation of these data. If it is possible to interpolate between such curves, then graphs or tables could be prepared to assign a definite index of effectiveness for a given set of operating conditions.

APPENDIX A: Symbols.

A	Amplitude ratio of output-to-input signal
a	Calibration constant---measure of damping---G/I
b	Calibration constant---measure of stiffness--H/I
D	Operator for differentiation with respect to time
$f\dot{\theta}$	Generator feedback
f_c	Critical damping
G	Coefficient of damping
$G(s)_o$	Open-loop transfer function
G(s)	Closed-loop transfer function
H	Forcing function
H(s)	Transfer function of feedback element
I	Inertia
i_p	Plate current
j	Complex operator
K	Closed-loop gain constant
K_a	Amplifier gain constant
K_m	Motor gain constant
K_g	Generator gain constant
k	Proportionality constant
L	Inductance
M_p	Maximum amplitude ratio
n	Gear ratio
R	Resistance
R_1, R_2	Roots of quadratic

r_p	Plate resistance
rpm	Revolutions per minute
s	Laplace operator
Syn	Synchronous
T	Time constant
T_e	Electrical time constant
T_m	Mechanical time constant
u	Amplifier gain
V_c	Control field voltage
θ	Angular displacement
$\dot{\theta}$	Output signal velocity
$\ddot{\theta}$	Output signal acceleration
θ_i	Input signal
θ_o	Output signal
ϕ	Phase angle between input and output signals
ψ	Angle of control surface displacement
ψ_o	Fixed control surface displacement
ω	Angular frequency in radians per second
ω_n	Undamped natural frequency
ζ	Damping ratio
μ	Amplification factor
$\sim$	Proportional to

APPENDIX B: Solution of the Equation of Motion.

The equation to be solved is

$$\ddot{\theta} + a\dot{\theta} + b\theta = 0$$

This equation must be solved subject to the condition of an initial displacement; i.e., at $t=0$, $\theta=\theta_o$, and $\dot{\theta}=0$.

Writing the equation in symbolic form using the operator($D=d/dt$) gives:

$$(D^2 + aD + b)\theta = 0$$

Therefore,

$$D = \frac{-a \pm \sqrt{a - 4b}}{2}$$

When $4b > a$, as is generally true,

$$D = -a/2 \pm i \sqrt{b - (a/2)^2} = -a/2 \pm i\omega$$

where $\omega = \sqrt{b - (a/2)^2}$

The solution is, therefore:

$$\theta = C_1 e^{(-a/2 + i\omega)t} + C_2 e^{(-a/2 - i\omega)t}$$

$$= e^{-a/2t}(C_1 \cos \omega t + C_2 \sin \omega t)$$

Using the first initial condition, that $\theta=\theta_o$ at $t=0$, gives : $C_1 = \theta_o$.

Similarly, the second initial condition gives: $C_2 = a\theta_o/2\omega$

The complete solution then becomes:

$$\theta = e^{-a/2\ t}(\theta_o \cos \omega t + a\theta_o/2\omega \sin \omega t)$$

From the relationship,

$$a\cos\phi + b\sin\phi = \sqrt{a^2 + b^2}\cos(\phi - \tan^{-1} b/a)$$

the equation becomes:

$$\theta = e^{-a/2\ t}\sqrt{\theta_o^2 + (a/2)^2\theta_o^2/\omega^2}\cos(\omega t - \beta)$$

where $\beta = \tan^{-1} a/2\omega$

Thus,

$$\theta = e^{-a/2\ t}\ \theta_o/2\omega\sqrt{4\omega^2 + a^2}\cos(\omega t - \beta)$$

and since $\omega = \sqrt{b - (a/2)^2}$

$$\theta = e^{-a/2\ t}\ \theta_o\sqrt{b}/\omega\ \cos(\omega t - \beta)$$

If, $\omega = \sqrt{b - (a/2)^2}$

$\omega^2 = b - (a/2)^2$

and $b = \omega^2 + (a/2)^2$

This relation may be represented as shown in the figure below:

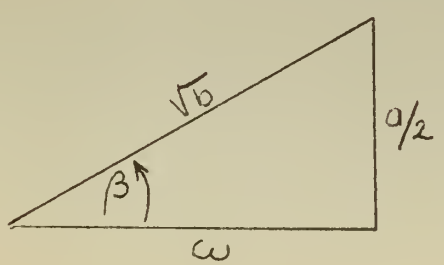

$\beta = \tan^{-1} a/2\omega$

From this figure, it may be seen that

$$\sqrt{b}/\omega = 1/\cos\beta$$

Thus,

$$\theta = \theta_o/\cos\beta\ e^{-a/2\ t}\ \cos(\omega t-\beta)$$

where $\omega = \sqrt{b-(a/2)^2}$

$\beta = \tan^{-1}\ a/2\omega$

The damped frequency of oscillation of the system can be stated as follows:

$$f = \omega/2\pi = \sqrt{b-(a/2)^2}/2\pi$$

BIBLIOGRAPHY

1. G. S. Brown and D. P. Campbell, Principles of Servomechanisms, John Wiley & Sons, Inc., New York, 1948.

2. Harold Chestnut and Robert W. Mayer, Servomechanisms and Regulating System Design, Vol. I, John Wiley & Sons, Inc., New York, 1951.

3. Henri Lauer, Robert Lesnik and Leslie E. Matson, Servomechanism Fundamentals, McGraw--Hill Book Co., Inc., New York, 1947.

4. M. F. Gardner and J. L. Barnes, Transients in Linear Systems, John Wiley & Sons, Inc., New York, 1947.

5. Lloyd O. Brown, Jr., "Transfer Function for a 2--Phase Induction Servo Motor", AIEE Technical Paper, 51-347.

6. "ARMA Induction Motors and Generators", Arma Corporation, Brooklyn, N. Y.

7. R. J. W. Koopman, "Operating Characteristics of 2-Phase Servomotors", AIEE Transactions, Vol. 68, New York, 1949.

8. "Brush Oscillograph Equipment Operating Information", Sections II and V, Brush Development Co., Cleveland.

9. R. V. Tiede, "Small Servo Induction Motors", Essay, The Johns Hopkins University, 1948.

10. Andrew Sobczyk, "Stabilization of Carrier-Frequency Servomechanisms", Journal of the Franklin Institute, Vol. 246, 1948.

11. "Statham Instruments", Bulletin No. 101, Statham Laboratories, Inc., Los Angeles.

VITA

Jack Leroy Miles was born in Clyde, Kansas, July 9, 1923. He graduated from Marysville High School, Marysville, Kansas, in 1941 and entered Fort Hays Kansas State College, Hays, Kansas, that same year. Early in 1942, he enlisted in the U. S. Marine Corps. In July, 1943, he was assigned to the Marine V-12 Unit at Purdue University, Lafayette, Indiana. Upon completion of the Platoon Commanders' School, Quantico, Virginia, he was commissioned a second lieutenant in the U. S. Marine Corps in June, 1945.

At the close of the war, he attended North Carolina State College, Raleigh, North Carolina, for a year before re-entering the U. S. Marine Corps in April, 1947. Assigned to the U. S. Naval Post Graduate School, Annapolis, Maryland, he completed the two year course in Guided Missile Guidance. On completion of the course in June, 1951, he was awarded the degree of Bachelor of Science in Electrical Engineering.

OCT 2
OCT 1
BINDERY
524

18050

Thesis
M585
Miles
An analysis of an electromechanical analogue computing system.
OCT 2
OCT 1
BINDERY
524

18050

Thesis
M585
Miles
An analysis of an electro-mechanical analogue computing system.

Library
U. S. Naval Postgraduate School
Monterey, California

thesM585
An analysis of an electrochemical analog
3 2768 000 98245 8
DUDLEY KNOX LIBRARY

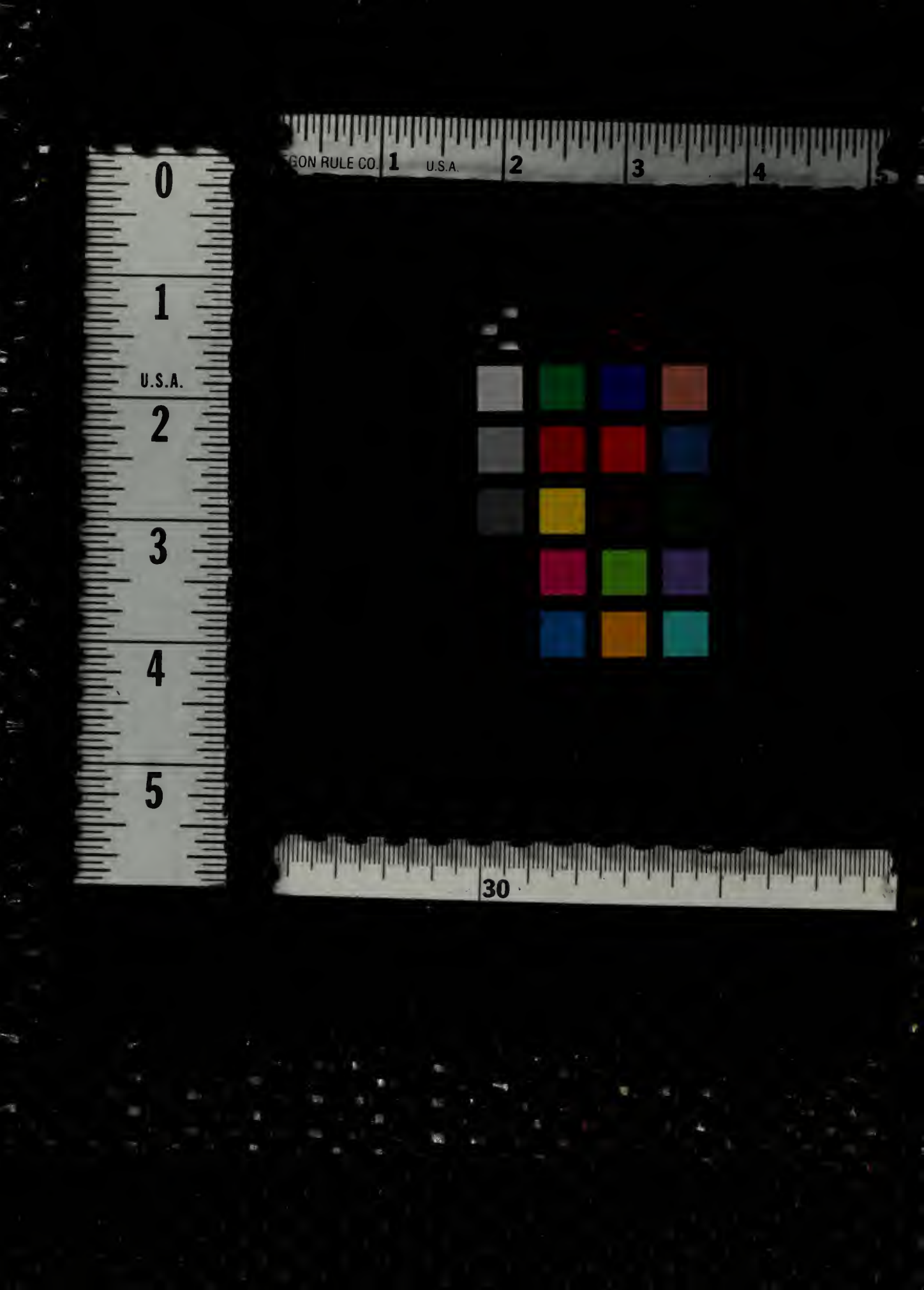
GON RULE CO.
1
U.S.A.
2
3
4
0
1
U.S.A.
2
3
4
5
30